RESEARCH ARTICLE

Sedimentary facies and mineral provenance of Upper Triassic sandstones offshore Kvitøya, Svalbard: implications for palaeogeographic interpretations in the northern Barents Shelf area

Mai Britt E. Mørk[1], Atle Mørk,[1] Sondre K. Johansen,[2] Kristian Drivenes[1,3] & Bjørn A. Lundschien[4]

[1]Department of Geoscience and Petroleum, Norwegian University of Science and Technology, Trondheim, Norway; [2]Norwegian Petroleum Directorate, Harstad, Norway; [3]The Geological Survey of Norway, Trondheim, Norway; [4]Norwegian Petroleum Directorate, Stavanger, Norway

Abstract

Upper Triassic (Carnian) sandstones of the De Geerdalen Formation cored south of the island of Kvitøya (80°N), north-easternmost Svalbard, are described in terms of sedimentary facies and petrography and compared regionally in the northern Barents Shelf. The succession off Kvitøya is characterized by its great thickness and is dominated by deltaic deposits with high sand content of lithic–feldspathic compositions. Comparison of sediment facies and sandstone compositions with adjacent areas suggest that the succession off Kvitøya is part of a larger delta system with its main sediment source from the east. The delta sedimentation was terminated by marine transgression in the earliest Norian. The sandstone compositions off Kvitøya differ from nearby locations by the higher content of cherty rock fragments and reworked volcanic debris in the Kvitøya sandstone, which is most distinct in the lower part of the succession. Provenance signatures are investigated by mineral–chemical analysis of detrital feldspars, rock fragments, garnet and Cr-spinel, characterizing a wide variety of igneous, metamorphic and sedimentary terranes, including palaeo-Urals and areas farther to east. Additional, more proximal sediment source areas may also have existed that could explain the increased sediment thickness and the mineralogical immature sandstone compositions of the Carnian sediments off Kvitøya.

Keywords
De Geerdalen Formation; Carnian; deltaic sedimentation; feldspar compositions; garnet; Cr-spinel

Correspondence
Mai Britt E. Mørk, Norwegian University of Science and Technology, Department of Geoscience and Petroleum, S. P. Andersens veg 15a, 7031 Trondheim, NO-7091, Norway. E-mail: mai.britt.mork@ntnu.no

Abbreviations
BEI: backscattered electron image
EDS: energy dispersive spectroscopy
EMP: electron microprobe
IGV: intergranular volume
NPD: Norwegian Petroleum Directorate
SEM: scanning electron microscope
XRD: x-ray diffraction

Introduction and geological setting

Provenance studies of sedimentary successions in the Barents Sea are important for palaeogeographic reconstructions and deciphering the sediment transport patterns throughout the geological history of today's Arctic region. During a drilling campaign offshore Kvitøya, in the northernmost Barents Sea (Fig. 1a), in 2015, the NPD collected shallow stratigraphic cores ranging in age from Carboniferous to Late Triassic, including a thick accumulation of Triassic sandstone-dominated sediments. The present study focuses on these Triassic sandstones that were cored south of Kvitøya in four locations less than 50 km apart (Fig. 1b, c). The Triassic sediments are correlated stratigraphically to the Upper Triassic De Geerdalen Formation defined in Svalbard and nearby offshore areas, and to the Snadd Formation defined in the south-western Barents Sea (Mørk et al. 1982; Worsley et al. 1988; Mørk et al. 1999; Riis et al. 2008; Lundschien et al. 2014; Vigran et al. 2014; Lundschien et al. 2023). A simplified stratigraphic overview is shown in Fig. 2. The Snadd–De Geerdalen formations represent the youngest part of the stratigraphy deposited in a giant north-west-prograding deltaic system. The delta system evolved from the south-east in the Early Triassic, possibly already in the latest Permian, to areas as far north as Svalbard in the Late Triassic (Bugge et al. 2002; Riis et al. 2008; Glørstad-Clark et al. 2010; Lundschien et al. 2014; Klausen et al. 2015; Gilmullina et al. 2021).

This paper describes the sedimentary succession of the De Geerdalen Formation in four stratigraphic cores off

Citation: *Polar Research* 2024, *43*, 9715, http://dx.doi.org/10.33265/polar.v43.9715

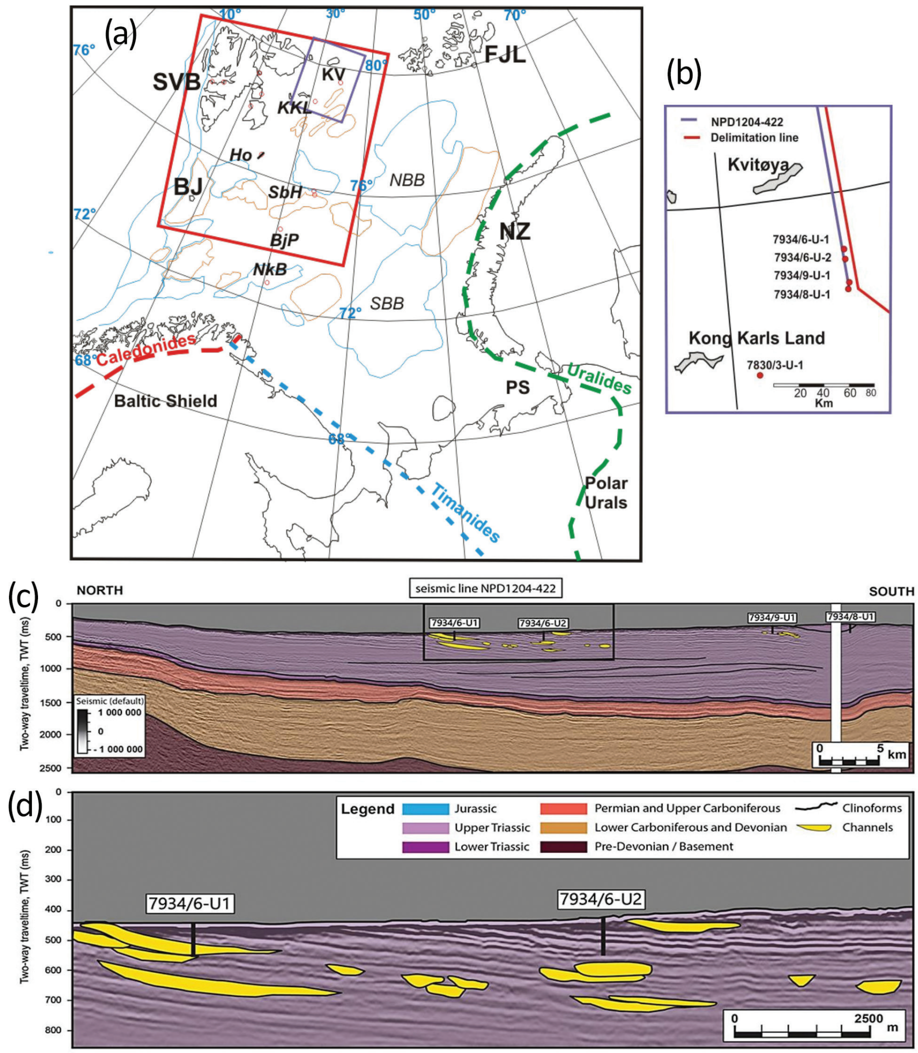

Fig. 1 (a) Barents Shelf overview, with structural elements modified from Smelror et al. (2009) and Gee et al. (2008). The red rectangle shows the area of the palaeogeographic maps in Fig. 13. (b) The location of NPD cores with Upper Triassic sediments off Kvitøya and nearby sites. (c) The seismic profile (NPD1204-422) off Kvitøya (KV) verifies the stratigraphic age relations between the cores. (d) A close-up of the interpreted channels in yellow (figure from NPD). Locations are specified in logs and palaeogeographic maps (Figs. 12, 13). Locations on the maps are as follows: Bjarmeland Platform (BjP), Hopen (Ho) and off Kong Karls Land (KKL), Nordkapp Basin (NkB) and Sentralbanken High (SbH). Other abbreviations: Svalbard (SVB), Bjørnøya (BJ), Novaya Zemlya (NZ), Franz Josef Land (FJL), Pechora Sea (PS), North Barents Basin (NBB) and South Barents Basin (SBB). Orange shows structural high.

Kvitøya and aims to identify sandstone distribution, sandstone provenance components and the use of facies distribution for palaeogeographic interpretation. The sedimentary succession is dominated by deltaic deposits, including shoreface, channel complexes and delta plain facies associations. These are comparable to the Carnian deposits in eastern Spitsbergen, Edgeøya and the Sentralbanken High. The succession and sandstone properties off Kvitøya are important for improving our understanding of sediment distribution and palaeogeography in the Late Triassic. Petrographic and mineral chemical analyses were performed to characterize sandstone properties, identify mineral provenance signatures and examine implications for regional geological provenance interpretations. The composite core section off Kvitøya is compared with sedimentary facies variations and available mineralogical data of the De Geerdalen and Snadd formations in Svalbard and nearby shallow cores offshore and is discussed in terms of sandstone provenance.

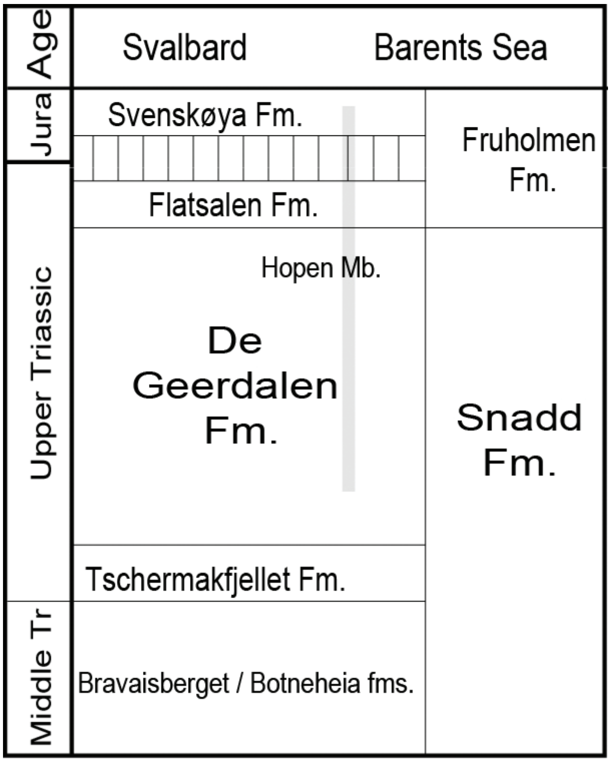

Fig. 2 The grey column in this simplified stratigraphic table marks the cores off Kvitøya that are discussed herein.

Sedimentary framework and depositional environments

The Upper Triassic sediments off Kvitøya are represented by cores in the wells 7934/6-U-1, 7934/-6-U-2, 7934/9-U-1 and 7934/8-U-1, shown in relation to the seismic line NPD-1204-422 in Fig. 1. The vertical thickness of the four cores covers a nearly continuous stratigraphic succession through the De Geerdalen Formation from the oldest core 6-U-1, except for minor gaps between the three lowermost cores and at the base (Fig. 3). The stratigraphically youngest cores—9-U-1 and 8-U-1—overlap. The thick sandstone-dominated De Geerdalen Formation is overlain by the Flatsalen Formation (mud dominated), which is overlain by the sandstones of the Svenskøya Formation in the upper part of core 8-U-1 (Fig. 3). Based on seismic interpretations, the accumulative thickness of the De Geerdalen Formation is ca. 600 m when also including the base of the formation, which is not cored. In comparison with Svalbard, a thickness of 650 m is estimated on the island of Hopen south-east of Spitsbergen (exposures, and Hopen-2 well; Lord, Solvi, Ask et al. 2014), and on Edgeøya only 250 m as the top is eroded. The formation has a maximum thickness of less than 350 m on Spitsbergen (Vigran et al. 2014; Lord et al. 2017). These observations suggest a westward thinning of the De Geerdalen Formation in Svalbard.

A lithostratigraphic compilation of the four cores off Kvitøya is shown in Fig. 3. The cores are characterized by sandstone and mudstone associations alternating at different scales and including frequent coal beds. The colour legend indicates a simplified grouping of the De Geerdalen Formation into deltaic, mostly delta plain deposits, channels or shoreface sandstones and mud-dominated shallow marine deposits. The deltaic plain deposits are characterized by thin bedded sandstone–mudstone and muddy sandstones with abundant mud clasts, often bioturbated. Synaeresis structures are particularly common in core 9-U-1 (Fig. 4h, i). Coal beds are common, and root structures often occur below the coal (Figs. 4f, j). The channel or shoreface deposits are represented by thicker sandstones. These include massive sandstones and sandstones with low angle cross-lamination. Such sandstones are mainly a few metres thick but may locally reach several tens of metres, as seen in the lower part of core 6-U-1 (Figs. 3, 4a, b, e). The shallow marine deposits are strongly bioturbated with diverse trace fossil content and marine fossils (Fig. 4a, d, c). The Flatsalen Formation, which overlies the De Geerdalen Formation, has abundant diverse bioturbation and beds with bivalves and represents more open marine depositional conditions (Fig. 3).

Core 6-U-1, the stratigraphically oldest core, displays bioturbated marine sandstones at the base, overlain by a thick succession (50 m) of sandstones (Fig. 4a). Coarse sandstone at the base fine upwards to medium sandstone with mud flakes. The remainder part of this sandstone is medium-grained and consists of beds with mud flakes at the base and lamina that are often rich in coal debris. Coal beds and beds with coal-shale are common in the upper part of the core, as well as root structures (Fig. 3). Cores 6-U-2 and 9-U-1 and the lower part of 8-U-1 show similar sedimentological facies of sandstones with thin coal seams, abundant roots and mudstone beds as in the uppermost part of core 6-U-1, but with a distinct facies transition to marine deposits with strongly bioturbated mudstone towards the top of the De Geerdalen Formation (Fig. 3). As suggested from seismic interpretation, a stratigraphic overlap between the lower part of core 8-U-1 and the upper part of core 9-U-1 is supported by the similar sedimentary facies.

The entire cored succession is interpreted to represent deposition in shallow marine and delta plain environments. The main facies of the three stratigraphic lower cores containing abundant thin coal beds, and coal beds with underlying roots are interpreted as vegetated delta plain environments (Fig. 3). The ca. 50 m thick sandstone succession in the lower part in core 6-U-1 is also visible in the

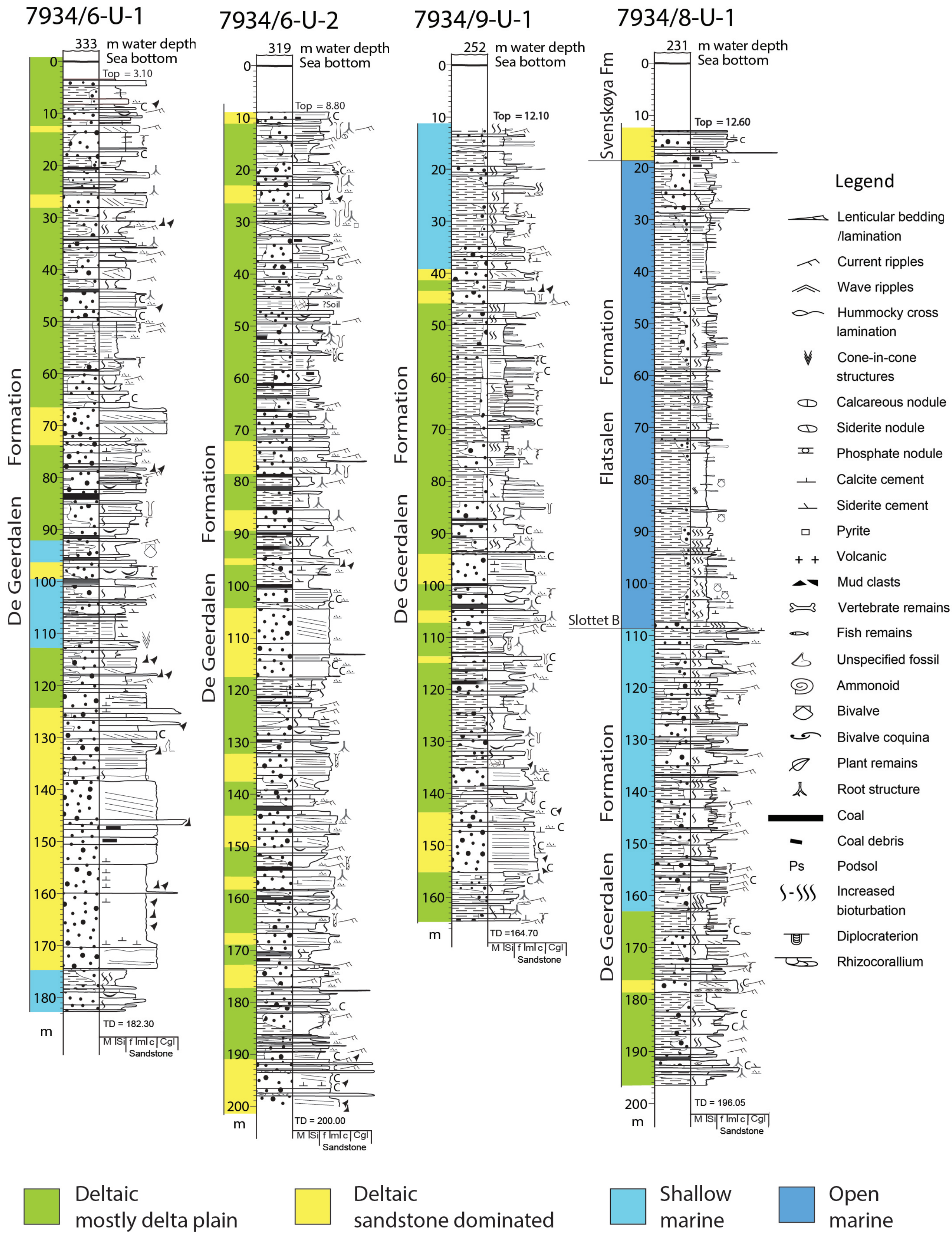

Fig. 3 Sedimentological logs of Triassic sediments in four different NPD shallow core locations off Kvitøya, arranged in accordance with stratigraphic age. Colours indicate a simplified facies division. See also core photographs (Fig. 4).

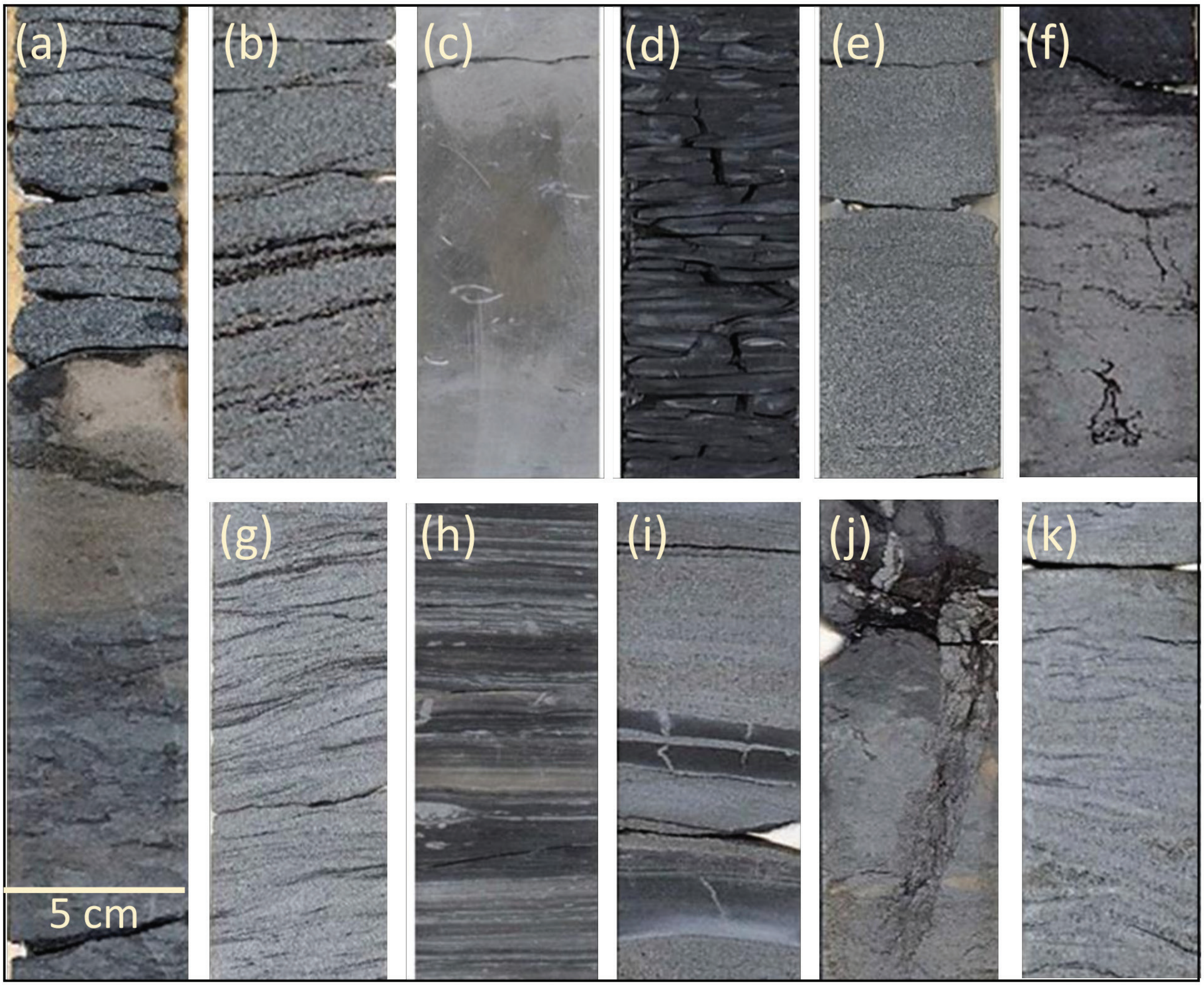

Fig. 4 Facies examples from NPD core photographs (depth numbers refer to image centre). 6-U-1: (a) shallow marine bioturbated muddy sandstone overlain by coarse sandstone, shoreface (174.2 m); (b) sandstone with lamina of coal debris (150.5 m); (c) carbonate-cemented bed with bivalves, inter-distributary bay deposit (110.7 m); (d) bioturbated mudstone and siltstone indicating marine condition (109.6 m); (e) massive to poorly laminated sandstone of channel/shoreface deposits (67.3 m). 6-U-2: (f) sandstone with roots below coalbed (61.5 m); (g) tidal channel (192.60 m). 9-U-1: (h, i) alternating mudstone–sandstone with syneresis structures in mudstone beds (77.8, 40.9 m). 8-U-1: (j) root structures below coalbed (191.6 m); (k) bioturbated, very fine-grained sandstone in the uppermost De Geerdalen Formation (110.5 m).

seismic section (Fig. 1c) and is interpreted as a channel complex. In the youngest core, 8-U-1, the change from delta plain sediments with sand beds including root structures and coal beds to mud-dominated sediments with increased bioturbation suggests increasing marine influence in the upper part of the formation. This part (163–109 m) strongly resembles the Hopen Member described and defined on the island of Hopen (Lord, Solvi, Ask et al. 2014), where shallow marine shales are capped by the transgressive Slottet Bed. This part of the stratigraphy differs from the development on Spitsbergen, where abundant red and green shales with podsols and thin coal beds of continental affinity are developed within upper delta plain deposits, for example, the Isfjorden Member (Lord et al. 2017; Lord et al. 2022). The uppermost part of the De Geerdalen Formation is missing on the islands of Edgeøya and Barentsøya, possibly because of late erosion (Lord, Solvi, Klausen et al. 2014; Lord et al. 2022). In eastern Spitsbergen, erosion at the Triassic–Jurassic transition is described by Klausen et al. (2022), and it is unknown if this erosion has also affected the eastern islands Edgeøya and Barentsøya.

Analytical methods

Sandstone mineral compositions and porosity in samples from the different stratigraphic levels were characterized using polished petrographic thin sections. Petrographic modal analysis was performed by optical microscopy, counting 300 points in each sample. Quantitative mineral–chemical analysis was performed using a Jeol JXF-8530F Plus electron microprobe at the Norwegian Laboratory for Minerals and Materials Characterization, Department of Geosciences and Petroleum, Norwegian University of Science and Technology. The acceleration voltage and beam current were set to 15 kV and 20 nA, respectively. Reference materials were natural minerals and pure metals by Astimex and Micro-Analysis Consultants. Very fine-grained rock fragments and accessory minerals were identified and characterized by combining backscatter imaging and EDS. The same thin sections were also used for estimation heavy mineral proportions by combining backscatter imaging and EDS mineral identification using a Hitachi SU6600 field emission gun SEM. Bulk-rock XRD analysis was performed to quantify plagioclase/K-feldspar ratios and supplement the mineral identification using a Bruker D8 advance with Co-source (λ1.78 Å, step size 0.011), scanning 2θ from 3 to 80°.

Sandstone petrography and porosity

The studied sandstone samples represent different facies and stratigraphic levels through the cored succession, covering shoreface, tidal flat and channel environments. The selected samples consist of fine- to medium-grained sands in the different settings, including the thick channel complex in the lower part of core 6-U-1, and sandstone beds ranging from ca. 1 m to several metres in thickness. The sandstones are characterized by well to moderate sorting and subangular–subrounded grains (Fig. 5). Finer-grained (silty–very fine) sandstones from delta plain and tidal flat environments are also examined.

Optical and electron microscopy shows similar sandstone mineralogy dominated by quartz, feldspar and cherty rock fragments in all parts of the formation (Figs. 6, 7, 8). Feldspar is abundant with both plagioclase and K-feldspar, whereas mica and detrital chlorite are present only in small amounts. The plagioclase/K-feldspar ratio estimated from the XRD analysis is approximately 2:1 throughout the formation (Fig. 7). Common accessory detrital heavy minerals observed in the petrographic thin-sections are garnet, Cr-spinel, apatite, rutile, zircon, ilmenite and, occasionally, tourmaline and staurolite. A possible stratigraphic variation in the proportion of the most frequent heavy minerals is shown in Fig. 9i, which indicates an increase in ilmenite and apatite in the upper part of the formation.

Polygranular rock fragments in the sandstones, in addition to the abundant chert grains, consist of altered volcanic rock fragments and fragments of very fine-grained sedimentary and metamorphic rocks. The volcanic rock fragments are recognized by randomly oriented

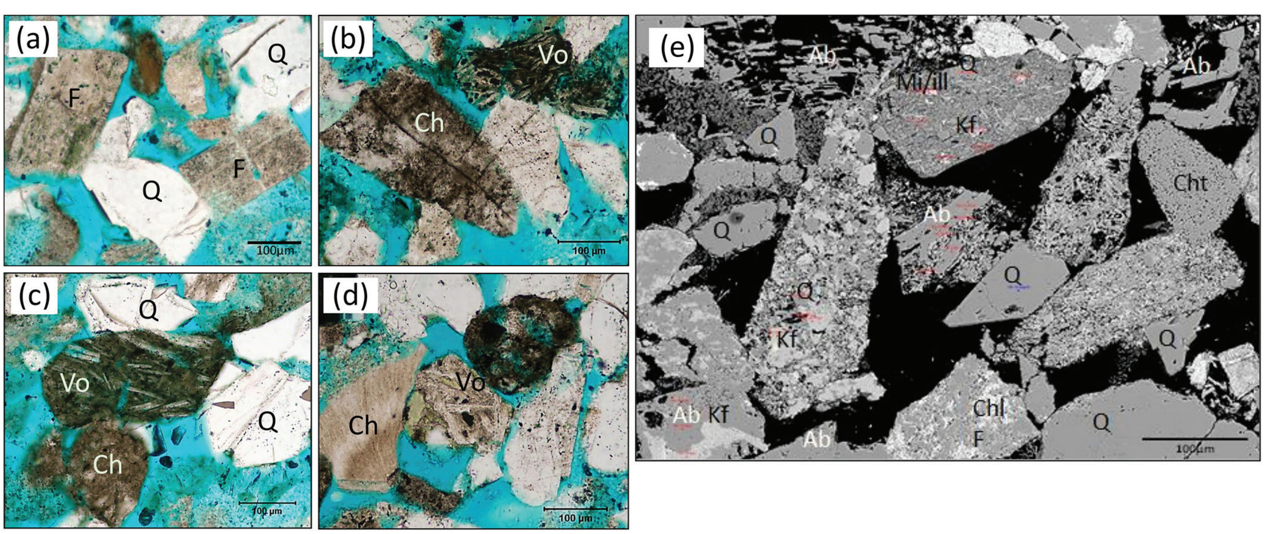

Fig. 5 Details of sample 6-U-1, 142.10 m rich in detrital rock fragments: (a-d) optical micrographs, blue indicating porosity. (a) Tabulate igneous feldspar (F) and quartz (Q) overgrown by angular quartz cement. (b) Chert (Ch) and volcanic rock fragment (Vo), the latter including thin feldspar laths. (c) Volcanic rock fragment, chert and quartz. (d) Vo shows feldspar laths with interstitial chlorite (green). (e) SEM BEI identifying detrital grains of mudstone, chert and chloritized and partly dissolved igneous rock fragments with albite (Ab). Black indicates porosity. Note net-like albite texture due to secondary dissolution at image top. Quartz, K-feldspar (Kf) and mica/illite (Mi/ill) are identified within the mudstone fragments.

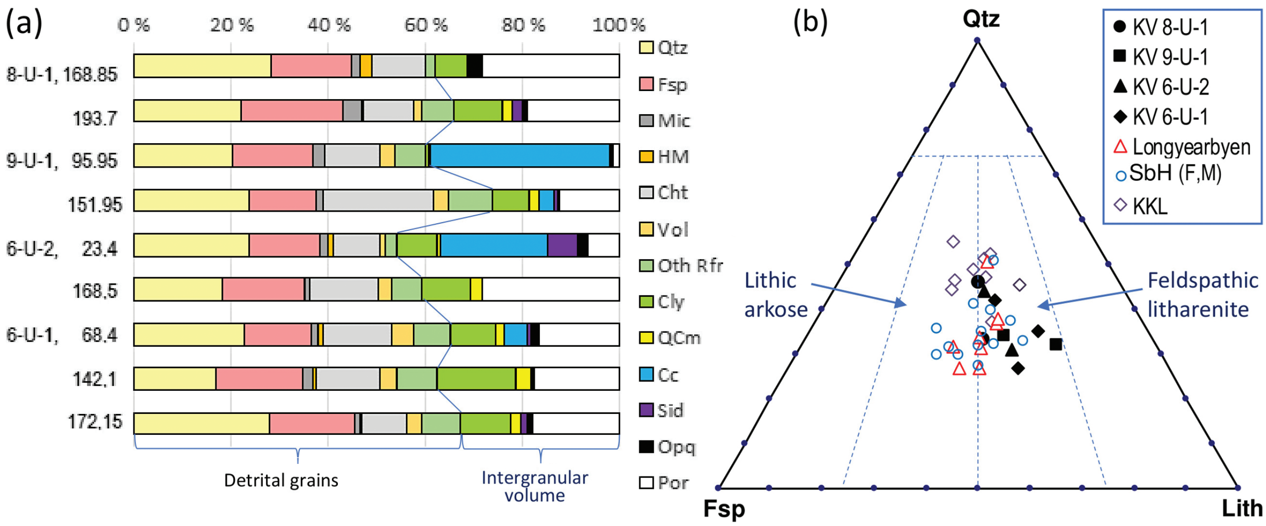

Fig. 6 Sandstone compositions off Kvitøya based on petrographic modal analysis. (a) Detrital grains: quartz (Qtz), feldspar (Fsp), mica (Mic), heavy minerals (HM), chert (Cht), volcanic fragment (Vol) and other rock fragments (oth). Diagenetic minerals: clay minerals (Cly), quartz cement (QCm), calcite (Cc), siderite (Sid) and opaques (Opq). Por = porosity. (b) Sandstone classification in terms of quartz, feldspar and lithics (Folk et al. 1970), and comparison with fine-medium-grained sandstones from Spitsbergen (Longyearbyen well Dh4) and shallow cores from the Sentralbanken High (7533/2-U-1, 7533/3-U-7) and off Kong Karls Land (7830/3-U-1).

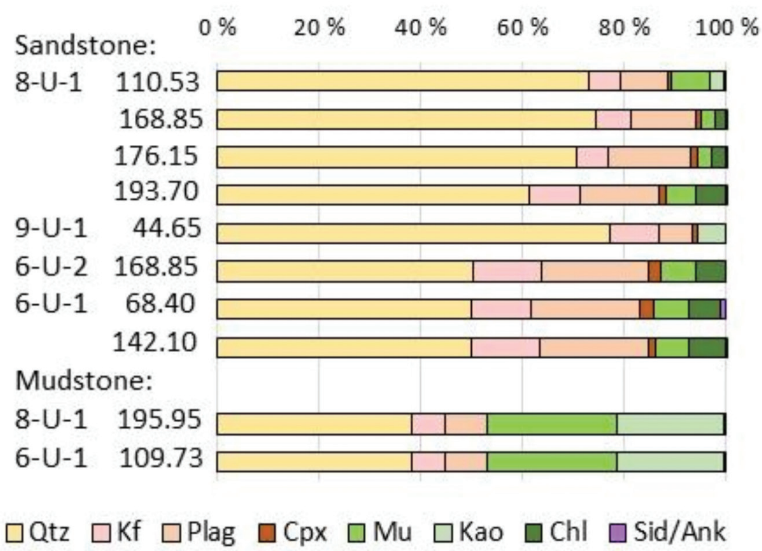

Fig. 7 Proportions (wt%) from XRD analyses of quartz (Qtz), K-feldspar (Kf), plagioclase (Plag), mica/illite (Mu), pyroxene (?) (Cpx), chlorite (Chl), kaolinite (Kao) and siderite/ankerite (Sid/Ank). The quartz includes mono- and polymineralic quartz, chert and cement.

feldspar laths enclosed in a dark or chloritized matrix (Figs. 5b–d). The variety of fine-grained fragment of chert, mudstone, quartz–feldspathic siltstone and altered volcanic fragments are documented in Fig. 5b–e from the lower channel sandstone. The mudstone fragments consist of clay with silt-sized particles of illite, mica, quartz and feldspar.

Sandstone classification based on petrographic modal analysis verifies mineralogical immature compositions, spreading between feldspathic lithic and lithic arkosic compositions (Folk et al. 1970; Fig. 6b). The compositions are comparable with sandstones from the De Geerdalen Formation in other locations in the northern Barents Sea (Riis et al. 2008) and Spitsbergen (Mørk

2013), overlapping with the most lithic sandstone compositions.

Diagenetic minerals

Diagenetic minerals in the samples include clay minerals, carbonate cement, minor quartz cement and occasional K-feldspar cement. Chlorite occurs as replacement of biotite, mafic rock fragments and glauconite, and rarely also as cement and coatings between clusters of grains. EMP analysis of chlorite within fine-grained volcanic rock-fragments shows Mg-chamosite composition. Illite is identified in mudstone rock fragments and as alteration products within feldspar. Kaolinite occurs both replacive within detrital grains, as pore-filling aggregates, and is also associated with partly dissolved feldspar grains. The localization of kaolinite aggregates in secondary dissolution pores lined by albite suggests a connection between plagioclase dissolution and crystallization of kaolinite. Kaolinite and mica/illite appear concentrated in interlayered mudstone (Fig. 7). Carbonate cemented beds sampled from shoreface and delta plain sandstones show cementation by pore-filling calcite (Fig. 6a). Very fine siderite cemented particles are commonly found associated with mud clasts. Ankerite and siderite are also detected as dispersed crystals in porous samples. Mn-rich siderite is particularly frequent in delta plain deposits near base of core 8-1, occurring as isolated crystals and in clusters with rhodochrosite cores. The latter is suggesting an origin from diagenetic alteration of root structures in palaeosols (e.g., Bojanowski et al. 2016). Authigenic K-feldspar was verified by SEM analysis in the lower part of core 6-U-1 (Fig. 8a, g, h). Quartz cementation is relatively limited in the samples off Kvitøya (Fig. 5a, c).

Porosity and IGV

Most of the sandstones appear loosely consolidated and show high porosity values in the channel facies. Petrographic modal analysis (Fig. 6a) shows porosity values between 28 and 13%, except in selected examples of strongly carbonate cemented beds (e.g., 5 and 1%). The high-porosity samples include moderately high intergranular porosity in combination with secondary dissolution porosity. The dissolution porosity is identified in skeletal feldspar remains and altered rock fragments (Fig. 5). The IGV defined by porosity + cement + matrix (Paxton et al. 2002) yields an average of 36%, which would suggest rather limited compaction. Subtracting visible dissolution porosity from the total porosity reduces the average IGV to 28%. This lower IGV value fits with petrographic evidence of compaction, exemplified by clusters with long grain contacts, and textures showing squeezing of ductile, altered and partly dissolved grains between rigid grains (Fig. 8b–d, g). The most compacted sample shows the highest content of chert and altered rock fragments (Fig. 6a).

Mineral chemical characterization

Electron microprobe analyses of detrital minerals were performed to characterize provenance signatures by the mineral chemistry of feldspars and the heavy minerals garnet and Cr-spinel. The samples selected for EMP analysis were chosen from different levels in the stratigraphically oldest and youngest cores, respectively, 6-U-1 and 8-U-1 (Fig. 3).

Feldspar

Plagioclase and K-feldspar may provide different information of provenance rock types on the basis of texture and chemical variation and degree of diagenetic alteration. The plagioclase analyses were performed on sand-sized grains as well as thin microliths in altered rock fragments. The plagioclase sand grains show albite (An0 – An9) and oligoclase (An14 – An18) compositions. The microliths in altered volcanic rock fragments (Fig. 5d, e) show relatively pure albite An0 – An3. The K-feldspar analysis shows mainly orthoclase-rich compositions with a range of Or73–Or100, with a high proportion of nearly pure K-feldspar. In combination with textural criteria (Fig. 8a, g–h), some of the most potassic compositions (>98% Or) are interpreted as authigenic overgrowths on the detrital K-feldspar (e.g., Kastner & Siever 1979; Milliken 1988; Parsons et al. 2005). Authigenic K-feldspar is also detected as fracture-fill in compacted Ba-rich K-feldspar (Fig. 8g).

In terms of interpreting provenance by combining mineral chemistry and feldspar texture, it is important to identify the type of igneous protolith. The present data refer to point analyses in homogeneous parts of feldspar grains avoiding visible albite lamellae if present. The studied K-feldspar grains range in texture from homogeneous to micro-perthitic, to perthitic feldspar with distinct albite lamellae and K-feldspar with distribution of fine or coarser patchy albite. Comparing analyses from available images show lowest Ab-content in K-feldspar that contains patchy albite inclusions, and higher values in homogeneous grains and micro-perthitic grains. The highest Ab-content is measured in Ba-rich K-feldspar in the channel complex in core 6-U-1.

Some K-feldspar grains show distinct variations in Ba-content. The analysed Ba-content in K-feldspar shows a

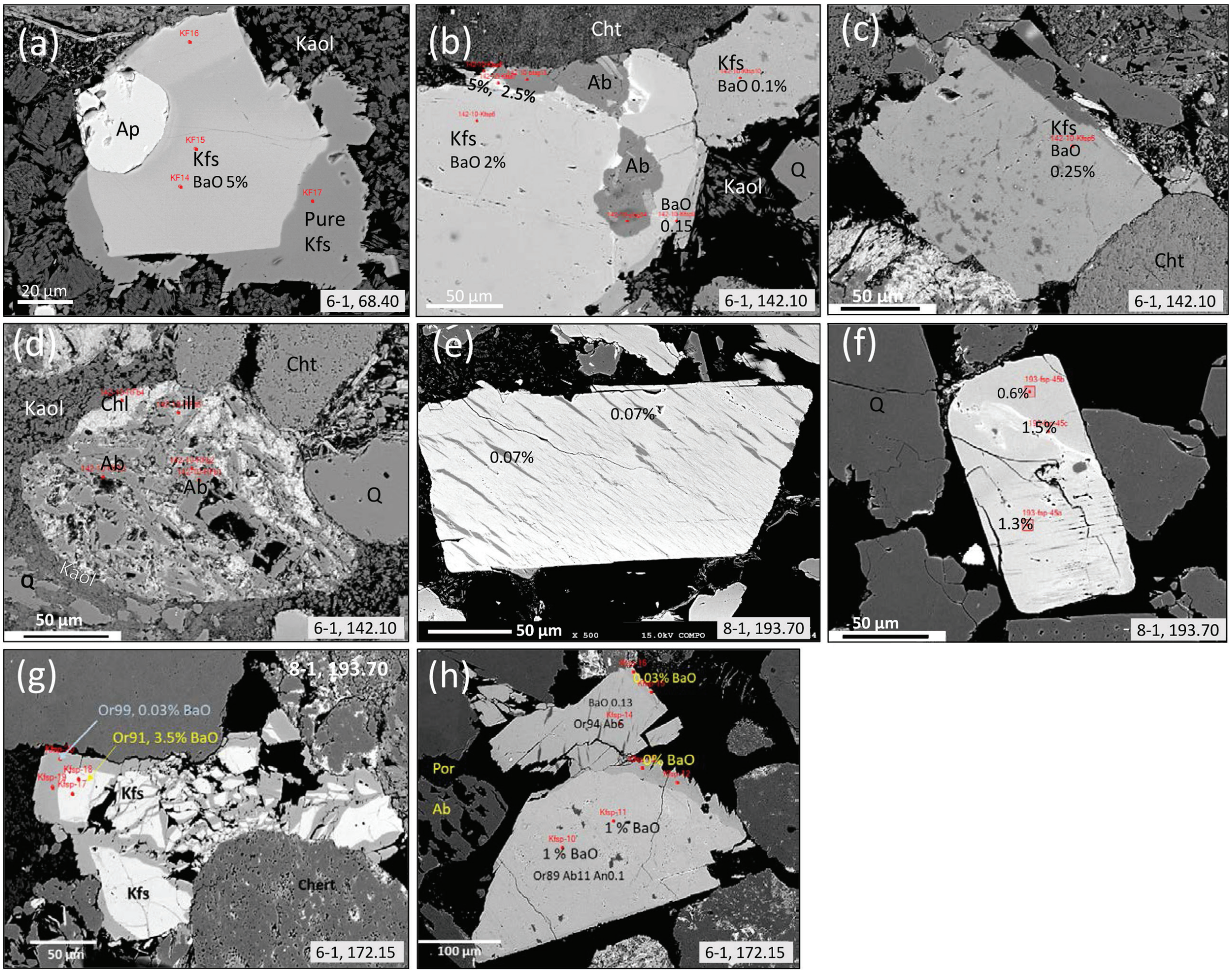

Fig. 8 BEI of K-feldspar, cores 6-U-1 and 8-U-1. Black indicates porosity. Numbers refer to wt% BaO. (a) Grain of Ba-rich K-feldspar intergrown with apatite, enclosed by K-feldspar cement. (b) Igneous rock fragment of Ba-rich K-feldspar (left) intergrown with albite (An_4). Other grains: Ba-poor feldspar, quartz (Q) and porous chert; authigenic kaolinite (Kaol) also visible. (c) K-feldspar with patchy albite inclusions. (d) Rock fragment with volcanic texture of thin albite laths (Ab), with interstitial chlorite (Chl) and minor kaolinite and illite. (e) Perthitic K-feldspar. (f) Subhedral K-feldspar with variation in BaO content. (g) Deformed and partly dissolved Ba-rich K-feldspar squeezed between quartz and chert grains. Relatively pure K-feldspar occurs as overgrowths and fracture-fill. (h) Fringy and smooth K-feldspar overgrowths on, respectively, Ba-rich homogeneous and Ba-poor perthitic feldspar. Note also partly dissolved albite (left).

total variation between 0 and 5.4 wt% BaO, thereby including Ba-feldspar and hyalophane (Deer et al. 2001). Excluding grains with BaO > 3% reduces the average composition to 0.4 wt% BaO. Occurrence of Ba-rich K-feldspar is detected at different stratigraphic levels and in polymineralic rock fragments (Fig. 8a, b). The Ba-rich detrital K-feldspar has been overgrown by Ba-poor K-feldspar of diagenetic origin.

Garnet

Garnet grains identified in the thin sections show considerable variation both in terms of shape and chemical composition. The analyses represent mostly very fine and fine-grained garnets, of either angular or sub-rounded shape, or idiomorphic crystals (Figs. 9a–c, g, h). The mineral chemical variation represented by endmembers pyrope (Pyr), almandine (Alm), spessartine (Sps) and grossular (Grs) is shown in Fig. 10. Most of the garnets have almandine-rich compositions (Alm_{60-80}), but with considerable variations in the proportions of Mg, Ca and Mn. The largest variation is in Mn-content, ranging from Mn-poor and Mn-rich almandine to spessartine garnets. Mn-rich garnets are detected both in the stratigraphically oldest core (6-U-1) and in the youngest core (8-U-1). The spessartine garnet occurs as very fine to fine poikilitic grains (Figs. 9g, h, 10a), and as homogeneous idiomorphic crystals ($Pyr_7Alm_{23}Sps_{53}Grs_{17}$; Fig. 9b). Notably, the poikilitic spessartine (Fig. 9h) contains inclusions of quartz and

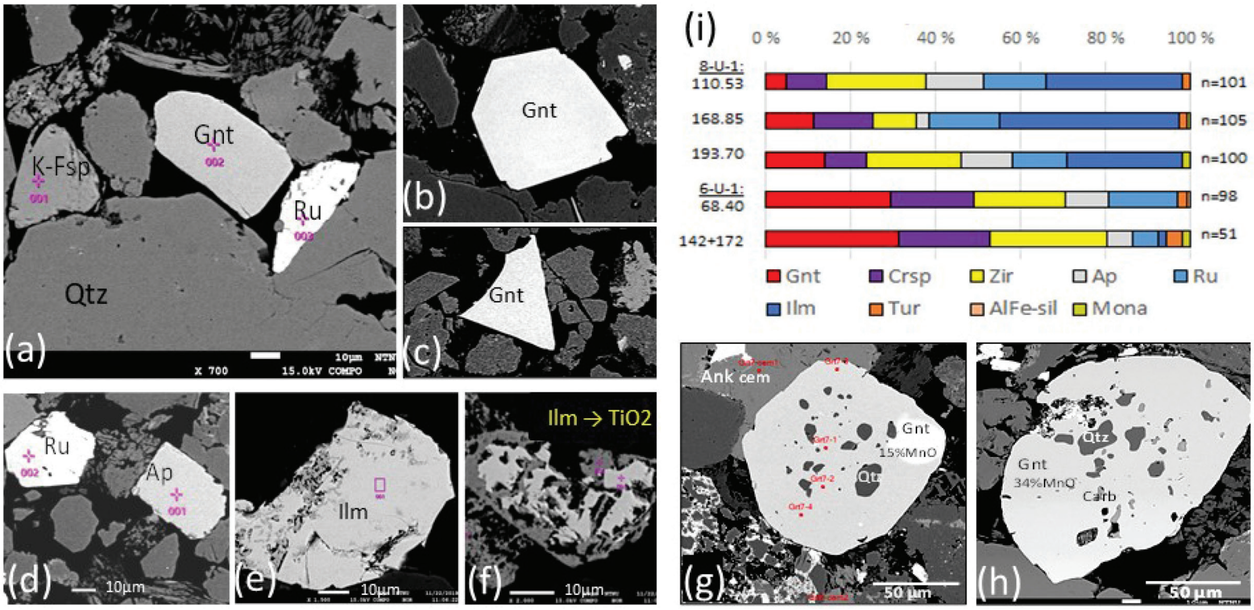

Fig. 9 BEI showing different garnet grain shapes (Gnt), (a-c) cores 8-1, 110.53 m and (g-h) poikilitic Gnt in core 6-U-1, 68.40 m. (d-f) Rutile (Ru), ilmenite (Ilm), apatite (Ap) and altered ilmenite in sample 8-1. (i) Detrital heavy mineral proportions based on point counting in thin sections using SEM-EDS in combination with BEI for mineral identification (n = number of counted grains). The heavy mineral grains range from coarse silt to very fine sand size. Garnet grains range up to fine-sand size. Accessory tourmaline is added from optical microscopy.

Mn-bearing carbonate. Figure 10b shows garnet compositions from shallow core locations in the central Barents Sea (Mørk 1999) for comparison with the present study, and Fig. 9c is included to illustrate Mn variation in garnets from south-eastern Barents Sea areas.

Cr-spinel

Chromium spinel occurs as a common accessory heavy mineral visible in all samples and is analysed in the thin-sections from cores 6-U-1 and 8-U-1. The compositions are characterized by low TiO_2 and a Cr_2O_3 range of 22–59 wt%, classifying as chromite and magnesio-chromite (Deer et al. 1965). An origin from ultramafic rocks is supported by plotting the element ratios Cr/(Cr+Al) – Mg/(Mg+Fe) (Fig. 11a) and by wt% TiO_2 – Al_2O_3 and wt% Cr_2O_3 – Al_2O_3 variations. The compositions are comparable with Cr-spinel in peridotite from ophiolite (Cookenboo et al. 1997; Fig. 11b) and with alpine type peridotites (Lenaz & Princivalle 2005). Similar Cr-spinel compositions are reported in ophiolites of the Voykar Massif, Polar Urals (Savelyev & Savelyeva 1979). Cr-spinel compositions reported from the De Geerdalen and the Snadd formations from different locations of the Barents Shelf from Svalbard to the Nordkapp Basin show considerable scatter in compositions in nearly all locations, but with a large majority of Cr-spinels of ophiolite signature (Harstad et al. 2021). The present Cr-Spinel data from channel sandstones off Kvitøya plot similarly to the data from the island of Hopen, south-east of Spitsbergen (Fig. 11).

In general, using Cr-spinel as a sediment provenance indicator is complicated, as considerable variations in Cr-spinel compositions may occur within the igneous protolith (Power et al. 2000). In addition, Cr-spinel compositions may also be influenced by metamorphic or metasomatic alteration of the source rocks (Kimball 1990; Bhat et al. 2019). Possible influences of chemical alteration in the present data are illustrated as a distinct increase in Fe and depletion in Al along intragranular fractures in the Cr-spinel grain displayed in Fig. 11.

Discussion

Mineral compositions and possible implications for provenance

Feldspar. Feldspar is one of the main minerals in sandstones, and their composition in combination with textures is useful in interpreting rock types and cooling history in source areas. Earlier studies of Triassic sandstone provenance in the western Barents Shelf noted a dominance of plagioclase over K-feldspar as part of mineralogically immature sediment components derived from the palaeo-Urals (Bergan & Knarud 1993; Mørk

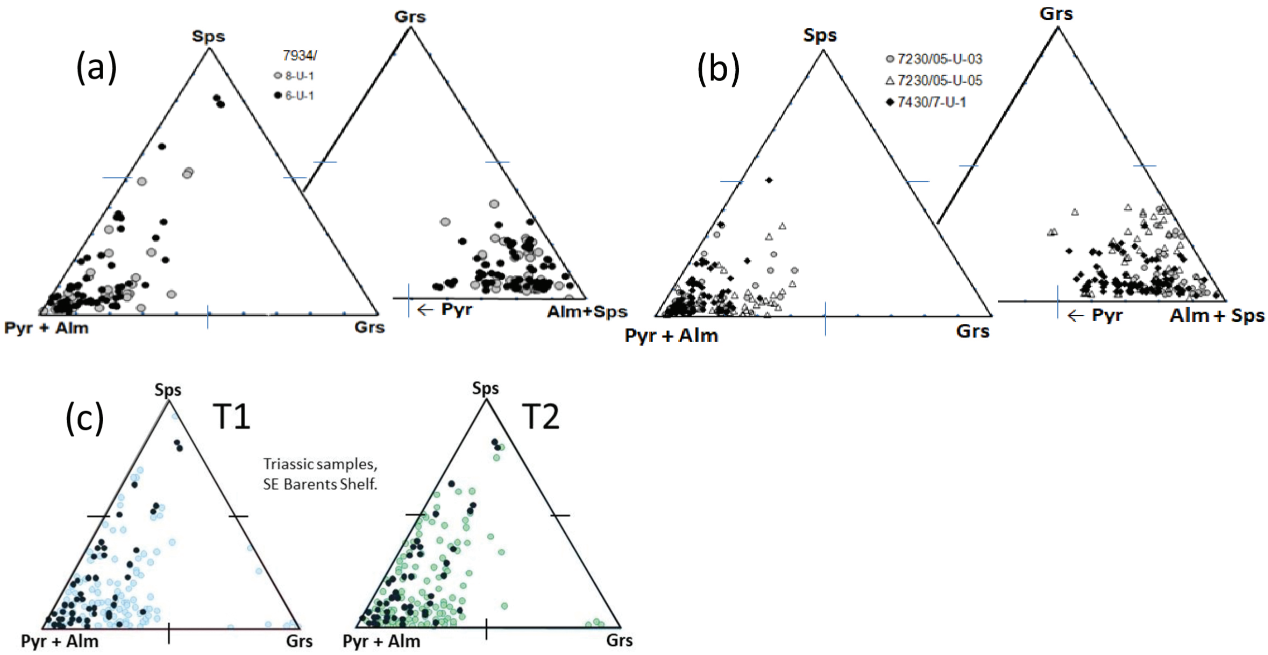

Fig. 10 (a) Garnet compositions (EMP analysis) in terms of endmembers, core 6-U-1 (samples 68, 142 and 172) and core 8-1 (samples 110, 168 and 193). Note large variation from Mn-poor almandines to nearly pure spessartine, and clustering of Alm + Sps compositions with variations in Ca and Mg contents up to 40%. (b) Shallow core data from the Snadd Formation in the Nordkapp Basin (NkB, 7230/3-U-5 and -U-3) and north at the Bjarmeland Platform (BjP, 7430/7-U-1; Mørk 1999) for comparison. (c) Garnet compositions (black dots) from de Geerdalen Formation sandstones off Kvitøya compared with garnets from Lower and Middle Triassic sandstones in south-eastern (Russian) areas in the Barents Sea. Modified from Mørk (1999).

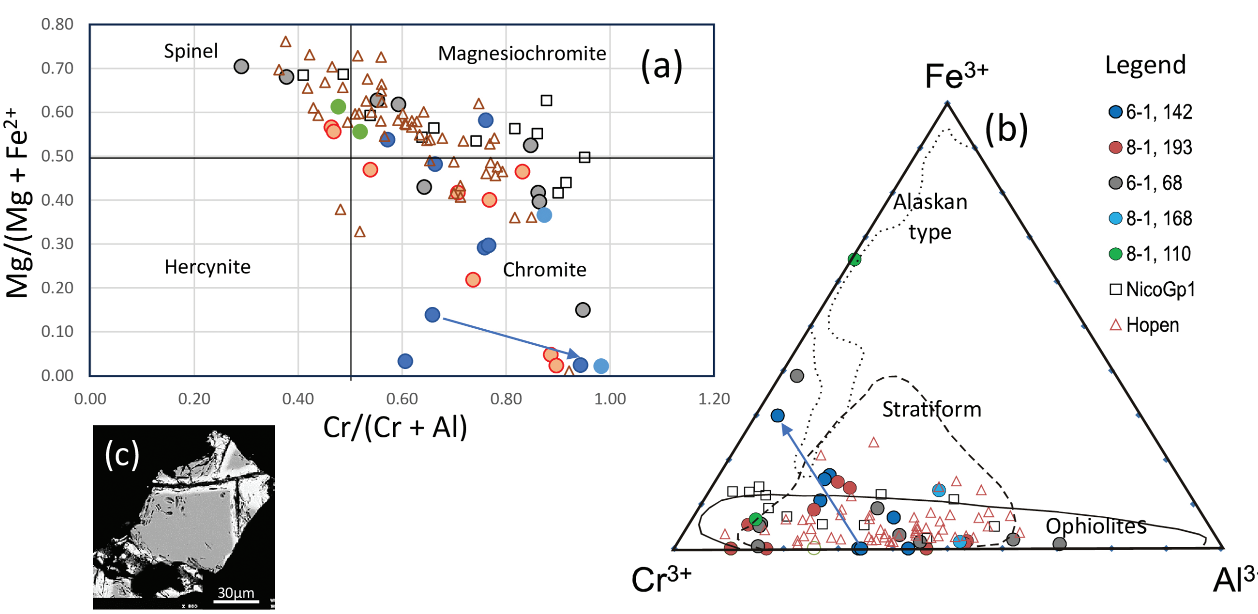

Fig. 11 Classification of Cr-spinel from EMP analysis of sandstones in cores 6-U-1 and 8-U-1. Arrows show the change in composition from igneous to altered chromite. Discrimination fields from (a) Schulze (2001) and (b) Cookenboo et al. (1997). Data from Hopen (Harstad et al. 2021) and north-east Siberia (Nikolenko et al. 2018; Gp1) are shown for comparison. (c) SEM-BEI of fractured Cr-spinel: bright colour shows Fe-enrichment and Al-depletion along the micro-fractures; see arrow in Fig. 11a, b (6-1, 142 m).

1999; Fleming et al. 2016; Line et al. 2018; Flowerdew et al. 2020). In the sandstones off Kvitøya, the variation in feldspar compositions would represent erosion of different igneous and meta-igneous rocks. As the plagioclase grains are dominated by albite, possible mafic source rocks would be of relatively low metamorphic grade, such as greenstone, as well as hydrothermally albitized rocks. The texture and mineral association of veryfine albite-chlorite intergrowths suggest an origin from basaltic volcanism for some of the volcanic debris. However, as albite and oligoclase are main minerals also in silicious igneous rocks and in low grade metamorphic rocks, different sources are possible for the sand-sized plagioclase grains. In addition, the significant content of magmatic K-feldspar indicates an intermediate or felsic source rock. A complicating factor in provenance interpretation is that albite may also form in diagenesis, commonly at temperatures above about 120 °C (Milliken 1988; Saigal et al. 1988), or by local heating of sediments from igneous activity (Haile et al. 2019). There is, however, no evidence of post-depositional albitization in the relatively porous De Geerdalen Formation sandstones off Kvitøya.

The textures and mineral chemistry of the detrital K-feldspar off Kvitøya show evidence of different sources. An origin from slowly cooled granite is suggested by the K-feldspar with fine perthitic exsolution textures (Fig. 8e, h). Grains that show irregular and patchy albite inclusions are also present (Fig. 8c), resembling hydrothermally altered igneous feldspar (e.g., Lee & Parsons 1997). A source from erosion of felsic plutonic rocks is supported by the assemblage Ba-rich K-feldspar, albite and apatite in igneous rock fragments (Fig. 8a, b). Ba-rich K-feldspar is known from crystallization of high-T granitoids (Smith 1974; Vernon 1986; Stimac & Pearce 1992; Zachariáš 2008). Figure 8b shows Ba-rich lining at crystal boundaries inside the igneous rock fragment. Similar features have been associated with late igneous processes involving hydrothermal infiltration of the igneous protoliths (Mehnert & Büsh 1981; Stimac & Pearce 1992; Zachariáš 2008). In total, the K-feldspar textures and chemistry reveal erosion of granitic rocks of different igneous history, and with different impacts from hydrothermal alteration in the source. These rock types would also have sourced much of the sodic plagioclase in the sandstones.

Garnet as a provenance indicator. Garnet compositions depend on bulk rock chemistry and metamorphic conditions of the source area and are a common tool in sandstone provenance studies (Morton 1987; Morton et al. 2004; Krippner et al. 2015; Fleming et al. 2016) often used as supplement to other methods. Almandine garnets with variation in Mn-Mg-Ca contents are widely distributed in metamorphic schists and gneisses. Spessartine garnets appear in Mn-rich sediments ranging from very low- to high-grade metamorphic conditions (Nyame et al. 1998; Makrygina & Suvorova 2011). Almandine-spessartine garnets are also described from granites and pegmatites, associated with late igneous or metasomatic crystallization (e.g., Kontak & Corey 1988; Stone 1988; Zachariáš 2008; Suggate & Hall 2013).

Garnet is considered relatively stable in diagenesis down to moderate burial depths, but with increasing burial Ca-richer, garnets are more easily dissolved (Morton 1987). The stability of garnet may also vary at shallow conditions, for example, associated with pyrite forming reactions (Zawidzka 2003). Secondary dissolution textures in garnet are also observed in siderite rich facies in the De Geerdalen Formation.

The compositions represented in the Alm+Sps – Pyr-Grs diagram (Fig. 10a) show a clustering of almandine-rich garnets with similar composition of Mg and Ca as Snadd Formation garnets at the Bjarmeland Platform and Nordkapp Basin (Fig. 10b). These compositions are also overlapping with garnets from exploration wells south-west in the Barents Sea (Fleming et al. 2016) with a main provenance signature of amphibolite facies metasedimentary rocks. In the present case, plots that separate Alm and Sps (Fig. 10a, b) are included to specify the large range in Mn-content of garnet in the samples off Kvitøya. Spessartine-rich garnets have earlier been described as common in Middle and Lower Triassic sandstones in samples from the south-eastern Barents Sea–Pechora Basin (Fig. 10c; fig. 7 in Mørk 1999) with interpreted source areas in the Palaeo Urals. The provenance may have included areas with Mn-rich metasediments like those described by Brusnitsyn et al. (2017) as common in the geology of the Polar Urals, Pay Koy and Novaya Zemlya.

Regional facies variation and palaeogeography

The studied De Geerdalen Formation off Kvitøya is compared with locations onshore Svalbard and shallow core locations in the northern Barents Sea (Fig. 12). Shallow stratigraphic cores off Kong Karls Land are closest to the present study area, whereas the Sentralbanken High is furthest away towards south-east. Colour codes in Fig. 12 show a generalized facies-grouping of open and shallow marine, deltaic and upper delta plain deposits.

Figure 12 also shows the transition from the underlying shale dominated Tschermakfjellet Formation, representing fully marine pro-delta environments, to the deltaic deposits of the Snadd–De Geerdalen formations.

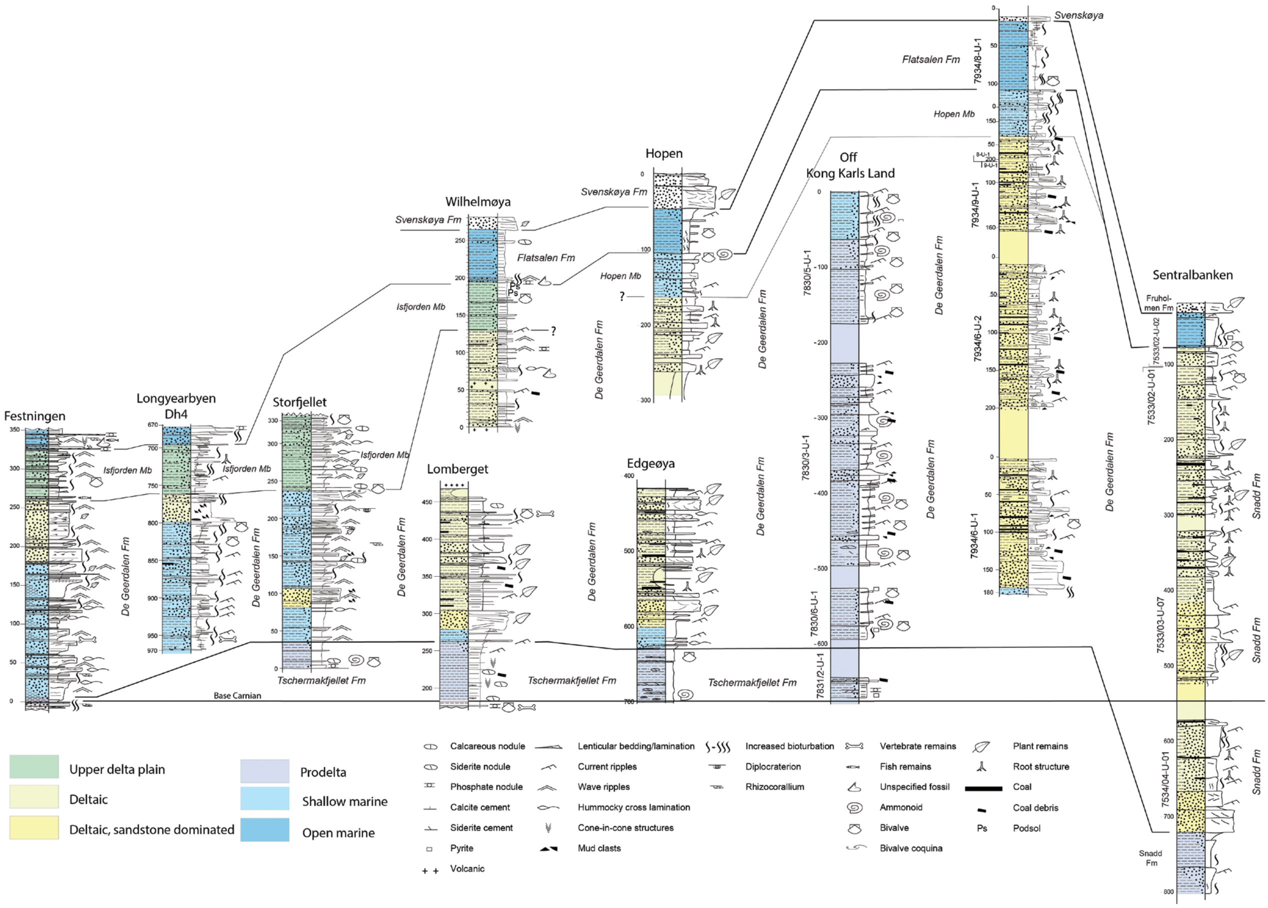

Fig. 12 Sedimentological logs comparing the off-Kvitøya cores with the surrounding areas. The log localities are presented in Fig. 13. The core logs are modified from Lundschien et al. (2014) and Vigran et al. (2014) and are correlated at the base Carnian (Late Triassic). Colours indicate a simplified facies division. It is unknown how much of the upper part of Edgeøya and Barentsøya and the area off Kong Karls Land is eroded, but the Hopen section is tentatively located above Edgeøya as indicated by the log thickness of the Hopen 2 well (Lord, Solvi, Ask et al. 2014).

This transition is gradual, with shaly marine deposits at Spitsbergen, Barentsøya and Edgeøya, but abrupt with deltaic sand deposits in the Sentralbanken High area. The cores off Kong Karls Land, located between the Sentralbanken High, the off-Kvitøya cores and the eastern Svalbard islands, show a succession that is more than 600 m thick, with abundant bivalves and ammonoids indicating open marine conditions. In the off-Kvitøya area, slightly north-west of the De Geerdalen Formation cores, another NPD core (7933/4-U-1; Lundschien et al. 2023) penetrates 75 m of the Tschermakfjellet Formation and includes *Halobia* sp. bivalves. On Spitsbergen, most of the De Geerdalen Formation is interpreted as shallow marine (Rød et al. 2014; Vigran et al. 2014), grading in the upper part to upper delta plain deposits (Lord et al. 2022). The islands east of Spitsbergen (Edgeøya, Barentsøya, Hopen, Wilhelmøya) not only are dominated by deltaic deposits with channels but also show beds with coal shale and minor interbeds of marine affinity with bivalves (Mørk et al. 1982; Klausen & Mørk 2014; Vigran et al. 2014; Lord et al. 2017; Haile et al. 2018; Paterson et al. 2019). The deltaic deposits off Kvitøya differ from the other locations by their greater thickness and higher sand content. The frequent intervals that contain root structures, coal beds and channels show a strong resemblance to the deltaic successions at the Sentralbanken High (Riis et al. 2008; Lundschien et al. 2014; Fig. 12).

The clearly deltaic sediments on the Sentralbanken High, off Kvitøya and on Hopen, Edgeøya and generally in eastern Svalbard contrast the fully marine succession off Kong Karls Land. The uppermost core off Kong Karls Land is dated as late early Carnian by Paterson et al. (2017) and includes a macrofauna with *Halobia* bivalves and ammonoids that is similar to the fauna in the Tschermakfjellet Formation. This may imply prodeltaic environments in front and between the delta lobes, and the great sediment thickness also implies large subsidence in this area. On the Kong Karls Land islands, the Late Triassic (Norian) Flatsalen Formation is fully marine (Olaussen et al. 2018).

The uppermost part of the De Geerdalen Formation in core 8-U-1 is interpreted as shallow marine, correlating to the Hopen Member on the island of Hopen (Fig. 12). This observation differs from the late development at Spitsbergen and Wilhelmøya, where upper delta plain sediments with occurrences of podsol layers and red and green shales of continental affinity (Isfjorden Member; Lord et al. 2022) are overlain by the Slottet Bed. Podsols are also present in the delta plain deposits in the middle part of the De Geerdalen Formation on Edgeøya (Haile et al. 2018; Lord et al. 2022) and below the Hopen Member on Hopen (Klausen & Mørk 2014; Lord, Solvi, Klausen et al. 2014). It is unknown how much of the upper part of Edgeøya and Barentsøya that is eroded.

Using interpretations from the correlation panels shown in Fig. 12, tentative palaeogeographic maps for Early, Mid and Late Carnian sections of the De Geerdalen Formation are suggested (Fig. 13). The Early Carnian map shows that at this time, the northern part of the Barents Shelf was covered by a large sea, and that continental sediments prograded towards the north-west from the south-east, as documented by multiple authors (Riis et al. 2008; Glørstad-Clark et al. 2010; Lundschien et al. 2014; Klausen et al. 2019). The early Carnian deposits are represented by marine prodelta shales of the Tschermakfjellet and lowermost De Geerdalen formations on Spitsbergen, Edgeøya and Barentsøya and off Kong Karls Land. The thick lower Carnian succession off Kong Karls Land implies major subsidence in this area. Marine deposition was also the case at Bjørnøya farther south (Mørk et al. 1990), whereas the Sentralbanken High area was characterized by mid to upper delta plain conditions (Riis et al. 2008).

The depositional change into the mid-Carnian is gradational. The delta complex from the south-east prograded further north-west, reaching the eastern islands of Svalbard and eastern Spitsbergen, while the north-western exposures of Spitsbergen show continued marine deposition. Deltaic conditions prevailed on the Sentralbanken High, in eastern Svalbard and off Kvitøya. Deltaic sediments with marine incursions are also described from time equivalent sediments far to the north-east, at Franz Josef Land (Preobranženskaja et al. 1985; Dypvik et al. 1998).

In the late Carnian, Spitsbergen was covered by deltaic deposits with upper delta top sediments rich in podsol beds with abundant red and green mudstones in the central and north-eastern areas extending north-east to Wilhelmøya (Lord et al. 2022). An area ranging from off Kvitøya, southward to Hopen was marine, possibly associated with increased subsidence. The Carnian succession is terminated by the latest Carnian/early Norian transgression depositing the Slottet Bed of the Flatsalen Formation (Mørk et al. 1999), initiating open marine deposition over the northern Barents Shelf. The marine deposition in the overlying Flatsalen Formation is time equivalent to the Akkar Member of the Fruholmen Formation, originally defined in the Hammerfest Basin closer to the Norwegian mainland (Worsley et al. 1988; Vigran et al. 2014).

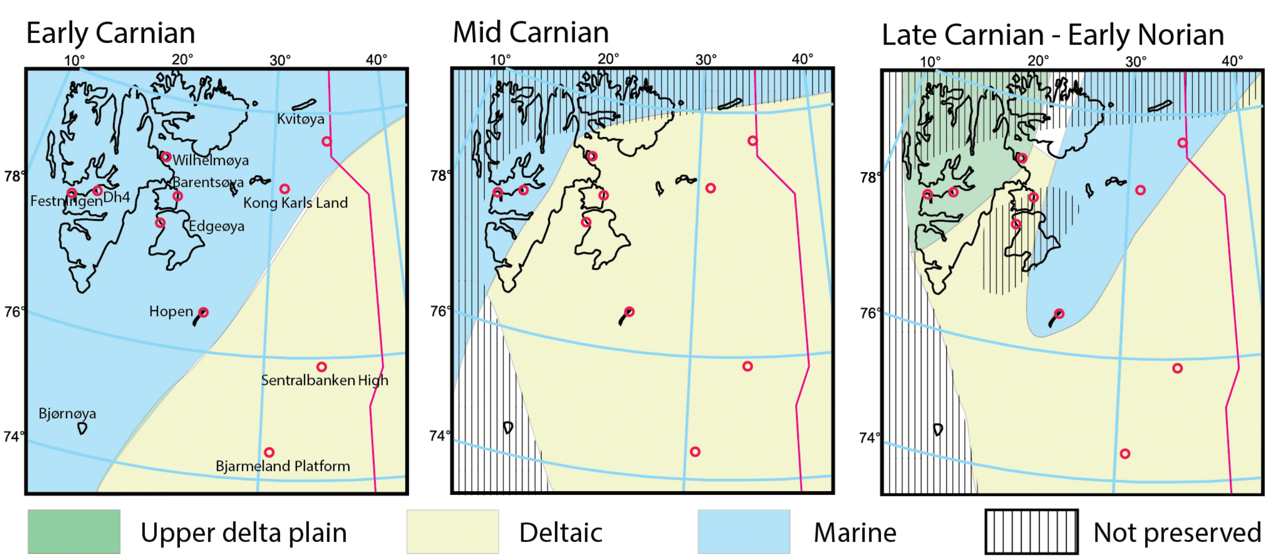

Fig. 13 Palaeogeographic interpretation for the northern Barents Shelf based on the correlation shown in Fig. 12.

Citation: *Polar Research* 2024, *43*, 9715, http://dx.doi.org/10.33265/polar.v43.9715

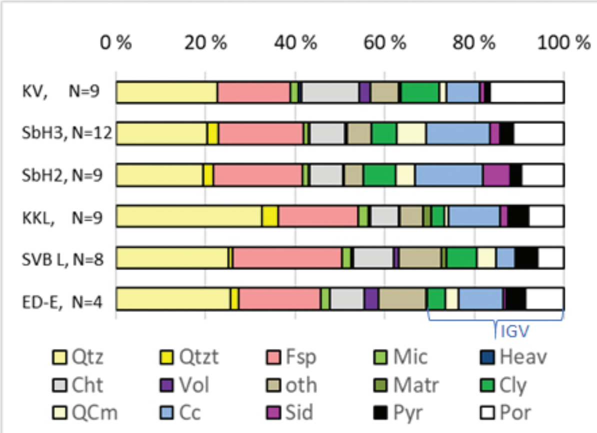

Fig. 14 Average sandstone compositions off Kvitøya (KV), Sentralbanken High (SbH cores 7533/3-U-7 and -/2-U-1), off Kong Karls Land (KK, core 7830/3-U-1), onshore in Longyearbyen, Spitsbergen (SVB-core Dh4) and exposure onshore on Edgøya (ED-BLA; Blanknuten), based on point count data of fine- to medium-grained De Geerdalen Formation sandstones. Mineral abbreviations as in Fig. 6.

Sandstone comparison

The sandstone compositions off Kvitøya are compared with similar facies of the De Geerdalen Formation on Spitsbergen (Longyearbyen, well Dh4), Edgeøya (Blanknuten) and the Sentralbanken High, and with the marine facies off Kong Karls Land (Riis et al. 2008; Mørk 2013; Figs. 12, 14). The sandstones are characterized by mineralogically immature compositions in all the studied locations (Figs. 6b, 14), except for a higher proportion of quartz in the marine deposits off Kong Karls Land. The sandstones off Kvitøya show the highest proportion of lithic grains of chert and volcanic debris. A comparison of average porosity shows the highest total porosity in the samples off Kvitøya (Fig. 14) and lowest values in the study from Spitsbergen (Longyearbyen, core Dh4), where porosity was greatly reduced by chemical compaction (Mørk 2013). Secondary dissolution porosity is, however, observed in thin sections from all the locations and appears most significant off Kvitøya and Kong Karls Land. The more compaction in the westernmost location would be in accordance with published models of net erosion across the Barents Shelf (e.g., Henriksen et al. 2011), resulting from variations in tectonics, burial and uplift history. Impacts on diagenesis from igneous intrusions may also be considered as Cretaceous dykes are widespread in the Triassic and Jurassic deposits in the northern Barents Shelf—the archipelago of Svalbard and offshore (Senger, Planke et al. 2014; Senger, Tveranger et al. 2014; Polteau et al. 2016; Olaussen et al. 2018; Haile et al. 2019). However, this would be most important close to intrusive contacts, which have not been observed in the present study.

Sandstone compositions and provenance

Earlier provenance studies in the western Barents Shelf have emphasized the palaeo-Urals (Uralides) as an important source for mineralogically immature Triassic sediment compositions (Bergan & Knarud 1993; Mørk 1999; Fleming et al. 2016; Line et al. 2018; Flowerdew et al. 2020). A south-eastern source was supported by seismic and sedimentological interpretations of north-westward deltaic progradation that was reaching parts of Svalbard in Late Triassic (Riis et al. 2008; Glørstad-Clark et al. 2010; Lundschien et al. 2014). Recent depositional models (Klausen et al. 2015; Klausen et al. 2019; Gilmullina, Klausen, Doré, Rossi et al. 2022; Gilmullina, Klausen, Doré, Sirevaag et al. 2022) suggest that the Late Triassic sedimentation was part of a Greater Barents Shelf Basin that extended from Siberia to Arctic Canada, with distant sediment sources in the Taimyr–Urals and the Central Asian Orogenic Belt. U-Pb dating of detrital zircon grains in the De Geerdalen and the Snadd formations and correlative formations revealed Hercynian (Uralian), Caledonian and Timanian zircon provenance ages in widespread areas of the Greater Barents Sea Basin (Miller et al. 2013; Pózer Bue & Andresen 2014; Soloviev et al. 2015; Fleming et al. 2016; Khudoley et al. 2019; Line et al. 2020; Klausen et al. 2022; Harstad et al. 2023). Detrital zircons of Permian-Mid Triassic age in the upper part of the formation compare with Siberian Trap and associated younger volcanism to the east (Reichow et al. 2009; Letnikova et al. 2014; Vernikovsky et al. 2020; Kurapov et al. 2021). The eastern provenance is supported also by Carboniferous zircon grain ages that compare with granite ages in areas far north-east and in Siberia (Lorenz et al. 2007; Vernikovsky et al. 2020). Caledonian and Late Precambrian ages are common in marginal basement provinces around the western Barents Sea as well as in nearby areas of the Triassic of Svalbard (Hjelle et al. 1978; Johansson et al. 2001; Terbenkov et al. 2002).

The studied mineralogy and petrography of the De Geerdalen Formation sandstones off Kvitøya suggest provenance from different areas and a variety of lithologies and variably altered and reworked volcanic debris. Mineral chemistry of K-feldspar, plagioclase, garnet and Cr-spinel demonstrates considerable variations both in igneous and metamorphic provenance signatures. The igneous components are derived from different types of granites and altered mafic rocks, and ultramafic rocks of ophiolitic affinity are supported by Cr-spinel compositions. A possible change in provenance, with depletion in volcanic and ultramafic components, is supported by variations in accessory heavy mineral proportions with a relative increase in ilmenite + apatite from the stratigraphic lower to the upper core off Kvitøya (Figs. 7, 9i).

As part of identifying sediment components of palaeo-Ural signatures, the sandstones off Kvitøya are also compared with earlier described Lower Triassic deposits from locations more proximal to the palaeo-Urals in the south-east, including the Pechora Sea. The proximal stratigraphic older deposits are dominantly of lithic compositions and dominated by rock fragments of greenstone, mafic volcanic debris, epidote and chert, as well as various sedimentary rock fragments (Ustritckij 1981; Pčelina 1988a, b; Mørk 1999). The Uralide provenance is also shown by Mn-rich garnet compositions in the Lower and Middle Triassic sandstones (Mørk 1999) in the south-eastern area. The frequency of similar provenance components in the much younger and more feldspar-rich samples as far away off Kvitøya is interesting. A possible interpretation is that the increased sediment deposition and subsidence off Kvitøya were receiving sediments from erosion of a northern extension of the Uralides (possibly north of Novaya Zemlya?) in the Carnian. The present study would also suggest that the Uralide provenance was decreasing in the upper part of the formation in association with periods of increased marine influence on the depositional environments in the late Carnian.

The comparison with Uralide components adds support to published models of eastern provenance for the Snadd–De Geerdalen formations (Fleming et al. 2016; Khudoley et al. 2019; Gilmullina et al. 2021). Considering the sandstone composition off Kvitøya, a mixed provenance that also explains the abundant sediment components from varied granitic source areas is probable. To investigate possible supplementary sources of short-transported igneous sediment components comparison with nearby igneous rocks exposed to the north, for example, on Nordaustlandet, Storholmen and Kvitøya (Flood et al. 1971; Lauritzen & Ohta 1984), would be of interest, assuming a larger extension of the igneous province in the past.

Conclusions

The De Geerdalen Formation off Kvitøya is characterized by high sand content and mineralogically immature sandstone compositions. Regional comparisons in the northern Barents Shelf show a dominance of deltaic sedimentation, developing from relatively open marine conditions lowermost in the formation to deltaic sedimentation in major parts of the area. The deltaic sedimentation was terminated by marine transgression from the north in the latest Carnian–earliest Norian.

The sandstone compositions off Kvitøya suggest a mixed provenance from terranes of mafic and felsic igneous rocks, metasedimentary rocks, volcanic debris, recycled sediments and cherts. Mineral associations and detrital mineral chemistry show evidence of slowly cooled granitoids, hydrothermally altered igneous rocks with Ba-rich feldspar and chloritized mafic igneous rocks. Additional provenance information is derived from garnet and Cr-spinel chemistry and variation in heavy mineral proportions in terms of ilmenite + apatite contents.

Comparison with previous studies supports contribution from eastern areas, possibly including a northern extension of the palaeo-Urals, and from reworked volcanic debris. The possibility of additional sediment contributions of more local provenance may also be suggested.

Acknowledgements

The authors acknowledge the NTNU laboratory staff, Laurentius Thijus, for performing the XRD analysis and Kjetil Eriksen for assistance with the SEM analysis. The authors also acknowledge several useful comments from the *Polar Research* reviewers Michael Flowerdew and Tore Grane Klausen. The authors specially acknowledge Tore for discussion and important comments on the correlations of the off Kong Karls Land cores.

Funding

This study was supported by NPD for sampling and laboratory analysis.

Disclosure statement

The authors declare no conflict of interest.

References

Bergan M. & Knarud R. 1993. Apparent changes in clastic mineralogy of the Triassic–Jurassic succession, Norwegian Barents Sea: possible implications for palaeodrainage and subsidence. In T.O. Vorren et al. (eds.): *Arctic geology and petroleum potential.* Pp. 481–493. Amsterdam: Elsevier.

Bhat I.M., Ahmad T. & Subba Rao D.V. 2019. Alteration of primary Cr-spinel mineral composition from the Suru Valley ophiolitic peridotites, Ladakh Himalaya: their low temperature metamorphic implications. *Journal of Earth System Science 128*, article no. 188, doi: 10.1007/s12040-019-1222-6.

Bojanowski M.J., Jaroszewicz E., Košir A., Łoziński M., Marynowski L., Wysocka A. & Derkowski A. 2016. Root-related rhodochrosite and concretionary siderite formation in oxygen-deficient conditions induced by a ground-water table rise. *Sedimentology 63*, 523–551, doi: 10.1111/sed.12227.

Brusnitsyn A.I., Kuleshov V.N., Perova E.N. & Zaitsev A.N. 2017. Ferromanganese carbonate metasediments of the Sob area, Polar Urals: bedding, conditions, composition, and genesis. *Lithology and Mineral Resources 52*, 192–213, doi: 10.1134/S0024490217030026.

Bugge T., Elvebakk G., Fanavoll S., Mangerud G., Smelror M., Weiss H.M., Gjelberg J., Kristensen S.E. & Nilsen K.

2002. Shallow stratigraphic drilling applied in hydrocarbon exploration of the Nordkapp Basin, Barents Sea. *Marine and Petroleum Geology 19*, 13–37, doi: 10.1016/S0264-8172(01)00051-4.

Cookenboo H.O., Bustin R.M. & Wilks K.R. 1997. Detrital chromium spinel compositions used to reconstruct the tectonic setting of provenance: implications for orogeny in the Canadian Cordillera. *Journal of Sedimentary Research 67,* 116–123, doi: 10.1306/d4268509-2b26-11d7-8648000102c1865d.

Deer W.A., Howie R.A. & Zussmann J. 1965. *Rock forming minerals. Vol. 5. Non-silicates*. New York: Longman.

Deer W.A., Howie R.A. & Zussmann J. 2001. *Rock forming minerals. Vol. 4A. Framework silicates: feldspars.* 2nd edn. London: The Geological Society.

Dypvik H., Sokolov A., Pcelina T., Fjellså B., Bjærke T., Korchinskaja M. & Nagy J. 1998. The Triassic succession of Franz Josef Land, stratigraphy and sedimentology of three wells from Alexandra, Hayes and Graham Bell islands. In A. Solheim et al. (eds.): *Geological aspects of Franz Josef Land and the northernmost Barents Sea. Norsk Polarinstitutt Meddelelser 151.* Pp. 50–82. Oslo: Norwegian Polar Institute.

Fleming E.J., Flowerdew M.J., Smyth H.R., Scott R.A., Morton A.C., Omma J.E., Frei D. & Whitehouse M.J. 2016. Provenance of Triassic sandstones on the southwest Barents Shelf and the implication for sediment dispersal patterns in northwest Pangaea. *Marine and Petroleum Geology 78*, 516–535, doi: 10.1016/j.marpetgeo.2016.10.005.

Flood B., Nagy J. & Winsnes T.S. 1971. *The Triassic succession of Barentsøya, Edgeøya and Hopen (Svalbard). Norsk Polarinstitutt Meddelelser 100*. Oslo: Norwegian Polar Institute.

Flowerdew M.J., Fleming E.J., Morton A.C., Frei D., Chew D.M. & Daly J.S. 2020. Assessing mineral fertility and bias in sedimentary provenance studies: examples from the Barents Shelf. In P. Dowey et al. (eds.): *Application of analytical techniques to petroleum systems.* Pp. 255–274. London: The Geological Society.

Folk R.L., Andrews P.B. & Lewis D.W. 1970. Detrital sedimentary rock classification and nomenclature for use in New Zealand. *New Zealand Journal of Geology and Geophysics 13,* 937–968.

Gee D.G., Fossen H., Henriksen N. & Higgins A.K. 2008. From the early Paleozoic platforms of Baltica and Laurentia to the Calédonie orogen of Scandinavia and Greenland. *Episodes 31*, 44–51, doi: 10.18814/epiiugs/2008/v31i1/007.

Gilmullina A., Klausen T.G., Doré A.G., Rossi V.M., Suslova A. & Eide C.H. 2022. Linking sediment supply variations and tectonic evolution in deep time, source-to-sink systems—the Triassic Greater Barents Sea Basin. *The Geological Society of America Bulletin 134*, 1760–1780, doi: 10.1130/B36090.1.

Gilmullina A., Klausen T.G., Doré A.G., Sirevaag H., Suslova A. & Eide C.H. 2022. Arctic sediment routing during the Triassic: sinking the Arctic Atlantis. *Journal of the Geological Society 180*, article no. jgs2022-018, doi: 10.1144/jgs2022-018.

Gilmullina A., Klausen T.G., Paterson N.W., Suslova A. & Eide C.H. 2021. Regional correlation and seismic stratigraphy of Triassic Strata in the Greater Barents Sea: implications for sediment transport in Arctic basins. *Basin Research 33*, 1546–1579, doi: 10.1111/bre.12526.

Glørstad-Clark E., Faleide J.I., Lundschien B.A. & Nystuen J.P. 2010. Triassic seismic sequence stratigraphy and paleogeography of the western Barents Sea area. *Marine and Petroleum Geology 27*, 1448–1475, doi: 10.1016/j.marpetgeo.2010.02.008.

Haile B.G., Czarniecka U., Xi K., Smyrak-Sikora A., Jahren J., Braathen A. & Hellevang H. 2019. Hydrothermally induced diagenesis: evidence from shallow marine deltaic sediments, Wilhelmøya, Svalbard. *Geoscience Frontiers 10*, 629–649, doi: 10.1016/j.gsf.2018.02.015.

Haile B.G., Klausen T.G., Czarniecka U., Xi K., Jahren J. & Hellevang H. 2018. How are diagenesis and reservoir quality linked to depositional facies? A deltaic succession, Edgeøya, Svalbard. *Marine and Petroleum Geology 92,* 519–546, doi: 10.1016/j.marpetgeo.2017.11.019.

Harstad T.S., Mørk M.B.E. & Slagstad T. 2021. The importance of trace element analyses in detrital Cr-spinel provenance studies: an example from the Upper Triassic of the Barents Shelf. *Basin Research 33*, 1017–1032, doi: 10.1111/bre.12502.

Harstad T.S., Slagstad T., Kirkland C.L. & Mørk M.B.E. 2023. Detrital zircon provenance of the vast Triassic Snadd and De Geerdalen formations, Barents Shelf, reveal temporal change in sediment source. *Norwegian Journal of Geology 103*, article no. 202308, doi: 10.17850/njg103-2-3.

Henriksen E., Bjørnseth H.M., Hals T.K., Heide T., Kiryukina T., Kløvjan O.S., Larssen G.B., Ryseth A.E., Rønning K., Sollid K. & Stoupakova A.V. 2011. Uplift and erosion of the greater Barents Sea. In A. Spencer et al. (eds.): *Arctic petroleum geology.* Pp. 271–281. London: The Geological Society.

Hjelle A., Ohta Y. & Winsnes T.S. 1978. The geology of northeastern Svalbard. *Norsk Polarinstitutt Årbok 1977*, 7–24.

Johansson Å., Maluski H. & Gee D.G. 2001. Ar-Ar dating of Caledonian and Grenvillian rocks from northeasternmost Svalbard—evidence of two stages of Caledonian tectonothermal activity in the High Arctic? *Norwegian Journal of Geology 81,* 263–281.

Kastner M. & Siever R. 1979. Low temperature feldspars in sedimentary rocks. *American Journal of Science 279,* 435–479.

Khudoley A.K., Sobolev N.N., Petrov E.O., Ershova V.B., Makariev A.A., Makarieva E.V., Gaina C. & Sobolev P.O. 2019. A reconnaissance provenance study of Triassic–Jurassic clastic rocks of the Russian Barents Sea. *GFF 141*, doi: 10.1080/11035897.2019.1621372.

Kimball K.I. 1990. Effects of hydrothermal alteration on the composition of chromian spinels. *Contributions to Mineralogy and Petrology 105,* 337–346, doi: 10.1007/BF00306543.

Klausen T.G. & Mørk A. 2014. The Upper Triassic paralic deposits of the De Geerdalen Formation on Hopen: outcrop analog to the subsurface Snadd Formation in the Barents Sea. *American Association of Petroleum Geologists Bulletin 98*, 1911–1941, doi: 10.1306/02191413064.

Klausen T.G., Nyberg B. & Helland-Hansen W. 2019. The largest delta plain in Earth's history. *Geology 47*, 470–474, doi: 10.1130/G45507.1.

Klausen T.G., Rismyhr B., Müller R. & Olaussen S. 2022. Changing provenance and stratigraphic signatures across the Triassic–Jurassic boundary in eastern Spitsbergen and the subsurface Barents Sea. *Norwegian Journal of Geology 102*, article no. 202205, doi: 10.17850/njg102-2-1.

Klausen T.G., Ryseth A.E., Helland-Hansen W., Gawthorpe G. & Laursen I. 2015. Regional development and sequence stratigraphy of the Middle to Late Triassic Snadd Formation, Norwegian Barents Sea. *Marine and Petroleum Geology 62,* 102–122, doi: 10.1016/j.marpetgeo.2015.02.004.

Kontak D.J. & Corey M. 1988. Metasomatic origin of spessartine-rich garnet in the South Mountain Batholith, Nova Scotia. *Canadian Mineralogist 26,* 315–334.

Krippner A., Meinhold G., Morton A.C. & Von Eynatten H. 2015. Heavy-mineral and garnet compositions of stream sediments and HP–UHP basement rocks from the Western Gneiss Region, SW Norway. *Norwegian Journal of Geology 96,* 7–17, doi: 10.17850/njg96-1-02.

Kurapov M., Ershovva V., Kudoley A., Luchitskaya M., Stockli D., Makariev A., Makarieva E. & Vishnevskaya I. 2021. Latest Permian–Triassic magmatism of the Taimyr Peninsula: new evidence for a connection to the Siberian Traps large igneous province. *Geosphere 17*, 2062–2077, doi: 10.1130/GES02421.1.

Lauritzen Ø. & Ohta Y. 1984. *Geological map of Svalbard 1:500 000, Sheet 4G, Nordaustlandet. Norsk Polarinstitutt Skrifter 154D.* Oslo: Norwegian Polar Institute.

Lee M.R. & Parsons I. 1997. Dislocation formation and albitization in alkali feldspars from the Shap granite. *American Mineralogist 82*, 557–570, doi: 10.2138/am-1997-5-616.

Lenaz D. & Princivalle F. 2005. The crystal chemistry of detrital chromian spinel from the southeastern Alps and outer Dinares: the discrimination of supplies from areas of similar tectonic setting? *The Canadian Mineralogist 43,* 1305–1314, doi: 10.2113/gscanmin.43.4.1305.

Letnikova E.F., Izokh A.E., Nikolenko E.I., Pokhilenko N.P., Shelestov V.O., Hilen G. & Lobanov S.S. 2014. Late Triassic high potassium trachitic volcanism of the northeast of the Siberian Platform: evidence in the sedimentary record. *Doklady Earth Sciences 459 Part 1,* 1344–1347, doi: 10.1134/S1028334X14110221.

Line L.H., Jahren J. & Hellvang H. 2018. Mechanical compaction in chlorite-coated sandstone reservoirs—examples from Middle–Late Triassic channels in the southwestern Barents Sea. *Marine and Petroleum Geology 96*, 348–370, doi: 10.1016/j.marpetgeo.2018.05.025.

Line L.H., Müller R., Klausen T.G., Jahren J. & Hellevang H. 2020. Distinct petrographic responses to basin reorganization across the Triassic–Jurassic boundary in the southwestern Barents Sea. *Basin Research 32*, 1463–1484, doi: 10.1111/bre.12437.

Lord G.S., Johansen S.K., Støen S.J. & Mørk A. 2017. Facies development of the Upper Triassic succession on Barentsøya, Wilhelmøya and NE Spitsbergen, Svalbard. *Norwegian Journal of Geology 97*, 33–62, doi: 10.17850/njg97-1-03.

Lord G.S., Mørk A., Haugan T., Boxaspen M.A., Husteli B., Forsberg C.S., Heggem B. & Olaussen S. 2022. Stratigraphy and palaeosol profiles of the Upper Triassic Isfjorden Member, Svalbard. *Norwegian Journal of Geology 102,* 202–215, doi: 10.17850/njg102-4-02.

Lord G.S., Solvi K.H., Ask M., Mørk A., Hounslow M.W. & Paterson N.W. 2014. The Hopen Member: a new member of the Triassic De Geerdalen Formation, Svalbard. *Norwegian Petroleum Directorate Bulletin 11*, 81–96.

Lord G.S., Solvi K.H., Klausen T.G. & Mørk A. 2014. Triassic channel bodies on Hopen, Svalbard: their facies, stratigraphic significance and spatial distribution. *Norwegian Petroleum Directorate Bulletin 11*, 41–59.

Lorenz H., Gee D. & Whitehouse M.J. 2007. New geochronological data on Palaeozoic igneous activity and deformation in the Severnaya Zemlya Archipelago, Russia, and implications for the development of the Eurasian Arctic margin. *Geological Magazine 144*, 105–125, doi: 10.1017/S001675680600272X.

Lundschien B.A., Høy T. & Mørk A. 2014. Triassic hydrocarbon potential in the northern Barents Sea; integrating Svalbard and stratigraphic core data. *Norwegian Petroleum Directorate Bulletin 11,* 3–20.

Lundschien B.A., Mattingsdal R., Johansen S.K. & Knutsen S.-M. 2023. North Barents composite tectono-sedimentary element. In S.S. Drachev et al. (eds.): *Sedimentary successions of the Arctic region and their hydrocarbon prospectivity.* London: The Geological Society.

Makrygina V.A. & Suvorova L.F. 2011. Spessartine in the greenschist facies: crystallization conditions. *Geochemical International 49,* 299–308, doi: 10.1134/S0016702911030074.

Mehnert K.R. & Büsch W. 1981. The Ba content of K-feldspar megacrysts in granites: a criterion for their formation. *Neues Jahrbuch für Mineralogie Abhandlungen 140*, 221–252.

Miller E.L., Soloviev A.V., Prokopiev A.V., Toro J., Harris D., Kuzmichev A.B. & Gehrels G.E. 2013: Triassic river-systems and the paleo-Pacific margin of northwestern Pangea. *Gondwana Research 23*, 1631–1645, doi: 10.1016/j.gr.2012.08.015.

Milliken K.L. 1988. Loss of provenance information through subsurface diagenesis in Plio-Pleistocene sandstones, northern Gulf of Mexico. *Journal of Sedimentary Petrology 58*, 992–2002, doi: 10.1306/212F8EE0-2B24-11D7-8648000102C1865D.

Mørk A., Dallmann W.K., Dypvik H., Johannessen E.P., Larssen G.B., Nagy J., Nøttvedt A., Olaussen S., Pchelina T.M. & Worsley D. 1999. Mesozoic lithostratigraphy. In W.K. Dallmann (ed.): *Lithostratigraphic lexicon of Svalbard, Upper Paleozoic to Quaternary bedrock. Review and recommendations for nomenclature use*. Pp. 127–214. Tromsø: Norwegian Polar Institute.

Mørk A., Knarud R. & Worsley D. 1982. Depositional and diagenetic environments of the Triassic and Lower Jurassic succession of Svalbard. In A.F. Embry & H.R. Balkwill (eds.): *Arctic geology and geophysics. Proceedings of the Third International Symposium of Arctic Geology*. Pp. 371–398. Calgary: Canadian Society of Petroleum Geologists.

Mørk A., Vigran J.O. & Hochuli P.A. 1990. Geology and palynology of the Triassic succession of Bjørnøya. *Polar Research 8,* 141–163, doi: 10.3402/polar.v8i2.6810.

Mørk M.B.E. 1999. Compositional variations and provenance of Triassic sandstones from the Barents Shelf.

Journal of Sedimentary Research 69, 690–710, doi: 10.2110/jsr.69.690.

Mørk M.B.E. 2013. Diagenesis and quartz cement distribution of low permeability Upper Triassic–Middle Jurassic reservoir sandstones, Longyearbyen CO_2 Laboratory well site in Svalbard, Norway. *American Association of Petroleum Geologists Bulletin 97*, 577–596, doi: 10.1306/10031211193.

Morton A., Hallsworth C. & Chalton B. 2004. Garnet compositions in Scottish and Norwegian basement terrains: a framework for interpretation of North Sea sandstone provenance. *Marine and Petroleum Geology 21,* 393–410, doi: 10.1016/j.marpetgeo.2004.01.001.

Morton A.C. 1987. Influences of provenance and diagenesis on detrital garnet suites in the Forties Sandstone, Paleocene, central North Sea. *Journal of Sedimentary Petrology 57,* 1027–1032, doi: 10.1306/212F8CD8-2B24-11D7-8648000102C1865D.

Nikolenko E.I., Logvinova A.M., Izokh A.E., Afanas'ev V.P., Oleynikov O.B. & Biller A.Y. 2018. Cr-spinel assemblage from the Upper Triassic gritstones of the northeastern Siberian Platform. *Russian Geology and Geophysics 59*, 1345–1361, doi: 10.1016/j.rgg.2018.09.011.

Nyame F.K., Kase K. & Yamamoto M. 1998. Spessartine garnets in a manganiferous carbonate formation from Nsuta, Ghana. *Resource Geology 48*, 13–22, doi: 10.1111/j.1751-3928.1998.tb00003.x.

Olaussen S., Larssen G.B., Helland-Hansen W., Johannessen E.P., Nøttvedt A., Riis F., Rismyhr B., Smelror M. & Worsley D. 2018. Mesozoic strata of Kong Karls Land, Svalbard, Norway; a link to the northern Barents Sea basins and platforms. *Norwegian Journal of Geology 98*, 1–69, doi: 10.17850/njg98-4-06.

Parsons I., Thompson P., Lee M.R. & Cayzer N. 2005. Alkali feldspar microtextures as provenance indicators in siliciclastic rocks and their role in feldspar dissolution during transport and diagenesis. *Journal of Sedimentary Research 75*, 921–942, doi: 10.2110/jsr.2005.071.

Paterson N.W., Mangerud G., Holen L.H., Landa J., Lundschien B.A. & Eide F. 2019. Late Triassic (early Carnian–Norian) palynology of the Sentralbanken High, Norwegian Barents Sea. *Palynology 43*, 53–75, doi: 10.1080/01916122.2017.1413018.

Paterson N.W., Mangerud G. & Mørk A. 2017. Late Triassic (early Carnian) palynology of shallow stratigraphical core 7830/5-U-1, offshore Kong Karls Land, Norwegian Arctic. *Palynology 41*, 230–254, doi: 10.1080/01916122.2016.1163295.

Paxton S.T., Szabo J.O., Ajdukiewicz J.M. & Klimentidis R.E. 2002. Construction of an intergranular volume compaction curve for evaluating and predicting compaction and porosity loss in rigid-grain sandstone reservoirs. *The American Association of Petroleum Geologists Bulletin 86*, 2047–2067, doi: 10.1306/61EEDDFA-173E-11D7-8645000102C1865D.

Pčelina T.M. 1988a. 6. Mezozojskie osadočnye kompleksy. 6.1. Triasovyj kompleks. 6.1. (6. The Mesozoic sedimentary complexes. 6.1. Triassic Complex.) In I.S. Gramberg (ed.): *Barencevskaja Šel'fovaja plita. (The Barents Shelf plate.)* Pp. 142–157. Leningrad: Nedra.

Pčelina T.M. 1988b. 9. Paleogeografija. 9.7. Triasovyj period. (9. Palaeogeography. 9.7 Triassic.) In I.S. Gramberg (ed.): *Barencevskaja Šel'fovaja plita. (The Barents Shelf plate.)* Pp. 211–218. Leningrad: Nedra.

Polteau S., Hendriks B.W.H., Planke S., Ganerød M., Corfu F., Faleide J.I., Midtkandal I., Svensen H.S. & Myklebust R. 2016. The Early Cretaceous Barents Sea Sill Complex: distribution, $^{40}Ar/^{39}Ar$ geochronology, and implications for carbon gas formation. *Palaeogeography, Palaeoclimatology, Palaeoecology 441,* 83–95, doi: 10.1016/j.palaeo.2015.07.007.

Power M.R., Pirrie D., Andersen J.C.Ø. & Wheeler P.D. 2000. Testing the validity of chrome spinel chemistry as a provenance and petrogenetic indicator. *Geology 28,* 1027–1030, doi: 10.1130/0091-7613(2000)28<1027:TTVOCS>2.0.CO;2.

Pózer Bue E. & Andresen A. 2014. Constraining depositional models in the Barents Sea region using detrital zircon U–Pb data from Mesozoic sediments in Svalbard. In R.A. Scott et al. (eds.): *Sediment provenance studies in hydrocarbon exploration and production.* Pp. 261–279. London: The Geological Society.

Preobraženskaja E.N., Škola I.V. & Korčinskaja M.V. 1985. Stratigrafija Triasovyh otloženij arhipelaga Zemlja Franca-Iosifa (po materialam parametričeskogo burenija). (Stratigraphy of the Triassic deposits of Franz Josef Land archipelago [on materials of parametric drilling].) In N.D. Vasyilevskaja (ed.): *Stratigrafija i paleontologija Mezozojskih osadočnyh vassejnov severa SSSR. (Stratigraphy and palaeontology of the Mesozoic sedimentary basins of the north of the USSR.*) Pp. 5–15. Leningrad: Research Institute of Arctic Geology.

Reichow M.K., Pringle M.S., Al'Mukhamedov A.I., Allen M.B., Andreichev V.L., Buslov M.M., Davies C.E., Fedoseev G.S., Fitton J.G., Inger S., Medvedev A.Y., Mitchell C., Puchkov V.N., Safonova I.Y., Scott R.A. & Saunders A.D. 2009. The timing and extent of the eruption of the Siberian Traps large igneous province: implications for the end-Permian environmental crisis. *Earth and Planetary Science Letters 277*, 9–20, doi: 10.1016/j.epsl.2008.09.030.

Riis F., Lundschien B.A., Høy T., Mørk A. & Mørk M.B.E. 2008. Evolution of the Triassic shelf in the northern Barents Sea region. *Polar Research 27*, 318–338, doi: 10.3402/polar.v27i3.6198.

Rød R.S., Hynne I.B. & Mørk A. 2014. Depositional environment of the Upper Triassic de Geerdalen Formation—an EW transect from Edgeøya to central Spitsbergen, Svalbard. *Norwegian Petroleum Directorate Bulletin 11*, 21–40.

Saigal G.C., Morad S., Bjørlykke K., Egeberg P.K. & Aagaard P. 1988. Diagenetic albitization of detrital K-feldspar in Jurassic, Lower Cretaceous and Tertiary clastic reservoir rocks from offshore Norway, I. Textures and origin. *Journal of Sedimentary Petrology 58*, 1003–1013.

Savelyev A.A. & Savelyeva G.N. 1979. Ophiolites of the Voykar Massif (Polar Urals). In J. Malpas & R.W. Talkington (eds.): *Ophiolites of the Canadian Appalachians and Soviet Urals. Memorial University of Newfoundland Geology Report 8.* Pp. 127–140. St Johns, NL: Memorial University of Newfoundland.

Schulze D.J. 2001. Origin of chromian and aluminous spinel macrocrysts from kimberlites in southern Africa. *Canadian Mineralogist 39*, 361–376, doi: 10.2113/gscanmin.39.2.361.

Senger K., Planke S., Polteau S., Ogata K. & Svensen H. 2014. Sill emplacement and contact metamorphism in a siliciclastic reservoir on Svalbard, Arctic Norway. *Norwegian Journal of Geology 94,* 155–169.

Senger K., Tveranger J., Ogata K., Braathen A. & Planke S. 2014. Late Mesozoic magmatism in Svalbard: a review. *Earth-Science Reviews 139*, 123–144, doi: 10.1016/j.earscirev.2014.09.002.

Smelror M., Petrov O.V., Larssen G.B. & Werner S.C. (eds.) 2009. *Atlas. Geological history of the Barents Sea.* Trondheim: Geological Survey of Norway.

Smith J.V. 1974*. Feldspar minerals. Vol. 2*. Berlin: Springer.

Soloviev A., Zaionchek A., Suprunenko O., Brekke H., Faleide J., Rozhkova D., Khisamutdinova A., Stolbov N. & Hourigan J. 2015. Evolution of the provenances of Triassic rocks in Franz Josef Land: U/Pb La-Icp-Ms dating of the detrital zircon from Well Severnaya. *Lithology Mineral Resources 50*, 102–116, doi: 10.1134/S0024490215020054.

Stimac J.A. & Pearce T.H. 1992. Textural evidence of mafic-felsic magma interaction in dacite lavas, Clear Lake, California. *American Mineralogist 77*, 795–809.

Stone M. 1988. The significance of almandine garnets in the Lundby and Dartmoor granites. *Mineralogical Magazine 52,* 651–658, doi: 10.1180/minmag.1988.052.368.09.

Suggate S.M. & Hall R. 2013. Using detrital garnet compositions to determine provenance: a new compositional database and procedure. In R.A. Scott et al. (eds.): *Sediment provenance studies in hydrocarbon exploration and production.* Pp. 373–394. London: The Geological Society.

Terbenkov A.M., Sandelin S., Gee D.G. & Johansson Å. 2002. Caledonian migmatization in central Nordaustlandet, Svalbard. *Norwegian Journal of Geology 82,* 15–28.

Ustritckij V.I. 1981. Triasovye i verchnepermskie otlozenija poluostrova Admiraltejstva (Novaja Zemlja). Triassic and Upper Permian deposits of the Admiralteystva Peninsula [Novaya Zemlya]). In D.S. Sorokov & Y.N. Kulakov (eds.): *Litologija i paleogeografija Barenceva i Karskogo morej. (Lithology and palaeogeography of the Barents and the Kara Sea*.) Pp. 55–65. Leningrad: Research Institute of Arctic Geology.

Vernikovsky V.A., Vernikovskaya A., Proskurnin V., Matushkin N., Proskurnina M., Kadilnikov P., Larionov A. & Travin A. 2020. Late Paleozoic–early Mesozoic granite magmatism on the Arctic margin of the Siberian craton during the Kara–Siberia oblique collision and plume events. *Minerals 10,* article 571, doi: 10.3390/min10060571.

Vernon R.H. 1986. K-feldspar megacrysts in granites—phenocrysts, not porphyroblasts. *Earth Science Review 23,* 1–63.

Vigran J.O., Mangerud G., Mørk A., Worsley D. & Hochuli P.A. 2014. *Palynology and geology of the Triassic succession on Svalbard and the Barents Sea.* Trondheim: Geological Survey of Norway.

Worsley D., Johansen R. & Kristensen S.E. 1988. The Mesozoic and Cenozoic succession of Tromsøflaket. In A. Dalland et al. (eds.): *A lithostratigraphic scheme for the Mesozoic and Cenozoic succession offshore mid- and northern Norway. Norwegian Petroleum Directorate Bulletin 4.* Pp. 42–65. Stavanger: Norwegian Petroleum Directorate.

Zachariáš J. 2008. Compositional trends in magmatic and hydrothermal silicates of the Petráčkova hora intrusive complex, Bohemian Massif—link between the magmatic processes and intrusion-related gold mineralization. *Journal of Geosciences 53*, 105–117, doi: 10.3190/jgeosci.021.

Zawidzka K. 2003. Behaviour of garnets in diagenesis of Cenozoic sedimentary rocks: examples from Poland. *Archiwum Mineralogiczne 54,* 99–112.